

We are IntechOpen, the world's leading publisher of Open Access books Built by scientists, for scientists

6,900

Open access books available

186,000

International authors and editors

200M

Downloads

Our authors are among the

154

Countries delivered to

TOP 1%

most cited scientists

12.2%

Contributors from top 500 universities



WEB OF SCIENCE™

Selection of our books indexed in the Book Citation Index
in Web of Science™ Core Collection (BKCI)

Interested in publishing with us?
Contact book.department@intechopen.com

Numbers displayed above are based on latest data collected.
For more information visit www.intechopen.com



Fatigue Endurance of Magnesium Alloys

Mariana Kuffová
Armed Forces Academy of General Milan Rastislav Štefánik
The Slovak Republic

1. Introduction

Magnesium alloys belong to the important light alloys. For wide utilization of Mg-alloys it is significant to know their properties, including the fatigue properties.

The fatigue of construction materials is a degradation process of irreversible changes in material properties caused by cyclic loading. Gradual accumulation of damage under repeated mechanical stress of the specimen, part of fabrication, known as the fatigue process, is conditioned by a great number of factors. Investigation of characteristics of the fatigue process depends on the kind of mechanical stress, the characteristic of testing machines and equipments. The criterion of material resistance to repeated stress is still the fatigue limit, expressed by the stress amplitude σ_a or the plastic deformation amplitude ε_{ap} under whose action material will endure an infinite number of cycles (fatigue limit σ_c), or at least a number of loading cycles determined in advance. The Wöhler curve in coordinates $\sigma_a - \log N$, or $\varepsilon_a - \log N$, is constructed on the basis of long-term tests of a great number of specimens. According to the respect of the fracture mechanics regularities, there is the dependence of fatigue crack growth on stress intensity factor ($da/dN = f(K_a)$) and threshold value of stress intensity factor K_{ath} . The importance of fatigue is tied foremost to safety of persons, which life is dependent on the reliability of given device operation (Nečas & Kelemen, 2010).

Cracks initiate and propagate from pre-existing flaws, material defects, or design features (fatter holes or sharp corners). In the fact, most fatigue is widespread, as hundreds, or even thousands of cracks are manifested in cyclic loading. The net effect of numerous fatigue cracks located in the same general area is that they synergistically interact reducing the structure's residual strength. However, the single-crack concept is still important, because ultimately, catastrophic failure can occur when a single crack goes critical and in the process envelops other adjacent cracks in zippering effect.

2. Available information about fatigue properties of magnesium alloys

Two basic methods are employed to predict and determine potential fatigue locations. The first is full-scale fatigue testing, which is performed during the development process. These tests are employed to ascertain the expected durability. Experimental fatigue tests can be performed under the low frequency cyclic loading, at frequencies to 2000 Hz (usually at $f \leq 200$ Hz) or under the high frequency cyclic loading ($f \approx 20$ kHz). In particular, fatigue tests are very expensive, since they require a lot of human and machine time. Using of high frequency cyclic loading allow us to obtain relevant information about fatigue endurance

and fatigue properties in areas of high and very high number of cycles ($N = 1.10^9 - 1.10^{12}$). Decreasing of expenses as well as increasing of efficiency of whole process of mechanical design and providing of operability during the overall lifetime of parts and machineries allow us to make progress in the field of the utilization of the computational technologies and the application of numerical methods for the solution of huge amount of mechanical engineering praxes' problems. Nowadays we have several commercial programs at our disposal which allow us to solve the crack propagation. Many authors have dealt with influence of the crack growth on the functionality of the particular parts from global point of view. Available simulation programs for the simulation of fatigue crack growth can be generally divided into numerical and analytical ones. The numerical programs (FRANC/FAM, FRANC3D, ADAPCRACK3D, CRACK-TRACER, ZENCRACK) are able to predict the crack path in arbitrary 2-D or 3-D structures by using the finite element or boundary element method, meshless method, the material point method. The lifetime is mostly calculated using linear damage accumulation. However, they are often very time consuming. On the other hand, analytical programs (NASGRO, ESACRACK, AFGROW) are very fast because no model has to be built, no meshing has to be done and the analysis is very rapid. But in many cases the analytical solutions for a number of selected problems do not match the real geometry and boundary conditions very well (Sander & Richard, 2006).

2.1 Fatigue endurance of magnesium alloys under low frequency cyclic loading

Fatigue tests for particular magnesium alloys were carried out by authors ((Bursk, 1997), (Cllaper & Watz, 1956), (Goodenberger, 1990)) to obtain relevant information about their fatigue endurance under low frequency cyclic loading. Their chemical composition and mechanical properties are shown in Tab. 1.

Alloy	Al	Zn	Mn	Cu	Si	Fe	Ni	Zr	Rm	Re	A
Wrought	[wt %]								[MPa]		[%]
AZ31B	3.0	1.0	0.2	-	-	-	-	-	260	200	15
AZ61A	6.5	1.0	0.15	-	-	-	-	-	310	230	16
ZK60A	-	5.5	-	-	-	-	-	0.4	305	205	16
AM503	0.01	0.01	1.62	0.02	0.006	0.007	0.003	-	200	107	6
Cast											
AZ63A	6.8	3.1	0.33	0.009	0.04	0.009	0.001	-	260	168	6,9
AZ91B	9.0	0.68	0.13	-	-	-	-	-	230	160	3
AZ91E	8.97	0.54	0.12	0.01	0.01	0.003	0.001	-	318	142	12

Table 1. Chemical composition and mechanical properties of particular magnesium alloys

Experimental fatigue tests were realised under different frequencies ($3.5 \div 50$ Hz), in air, at the temperature of surroundings and the criterion of failure was the final fracture. From the measured results, dependences applied stress – number of cycles, $\sigma_a = f(N)$, were plotted. The results for wrought and cast magnesium alloys are depicted in Fig. 1.

Fatigue limit σ_c of magnesium alloys has been determined in the range $70 \div 150$ MPa at the terminal number of cycles $N = 1.10^7$ cycles, Table 2 and Fig. 1.

During the experimental fatigue tests, the influence of particular factors on the fatigue lifetime was observed. The authors have noted that the fatigue endurance of magnesium alloys is influenced by surface conditions. Sharp notches, small radii, fretting and corrosion

are more likely to reduce fatigue life than variations in chemical compositions or heat treatment. Removing the relatively rough as-cast surfaces of castings by machining improves fatigue properties of the castings, what is depicted in Fig. 2 (Avedesian & Baker, 2000). The influence of the microstructure on fatigue lifetime is conditioned by homogeneity

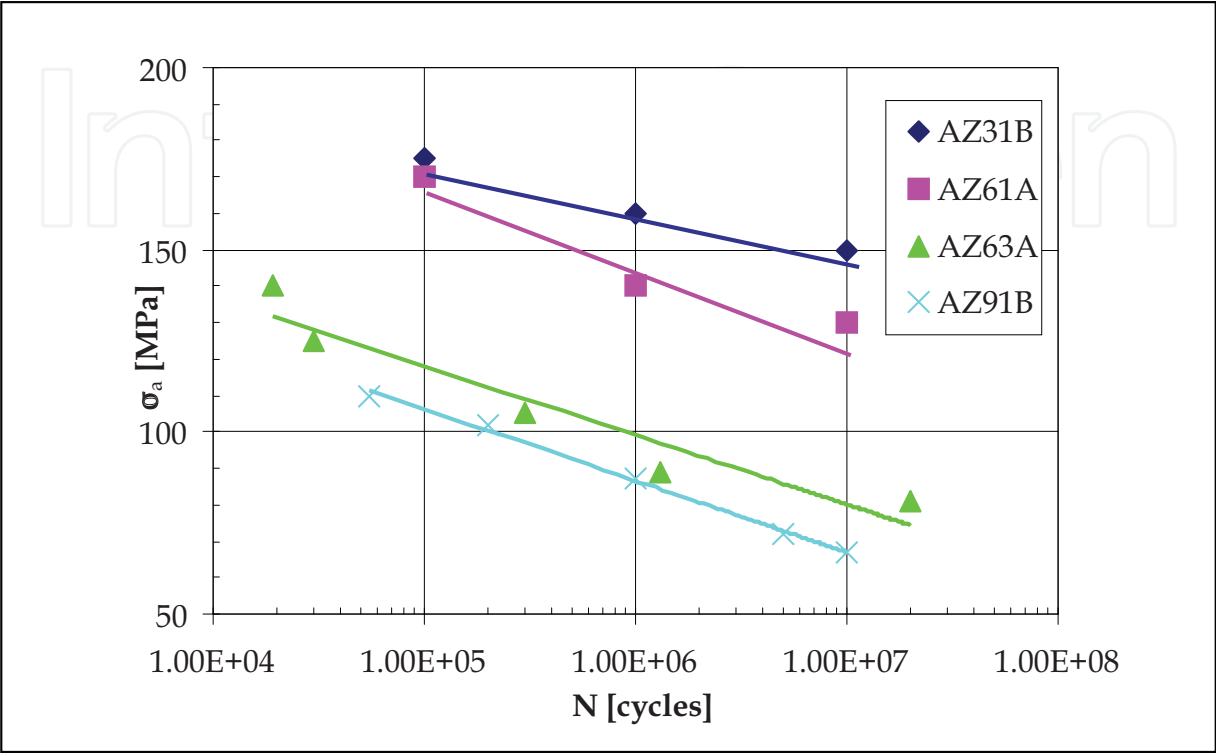


Fig. 1. Dependence $\sigma_a = f(N)$ of particular magnesium alloys

Mg - alloys	AZ 31B	AZ 61A	AZ 63A	AZ 91B
R	0.25	0.25	-1	-1
σ_c [MPa]	150	130	85	70

Table 2. Fatigue limit σ_c of particular magnesium alloys

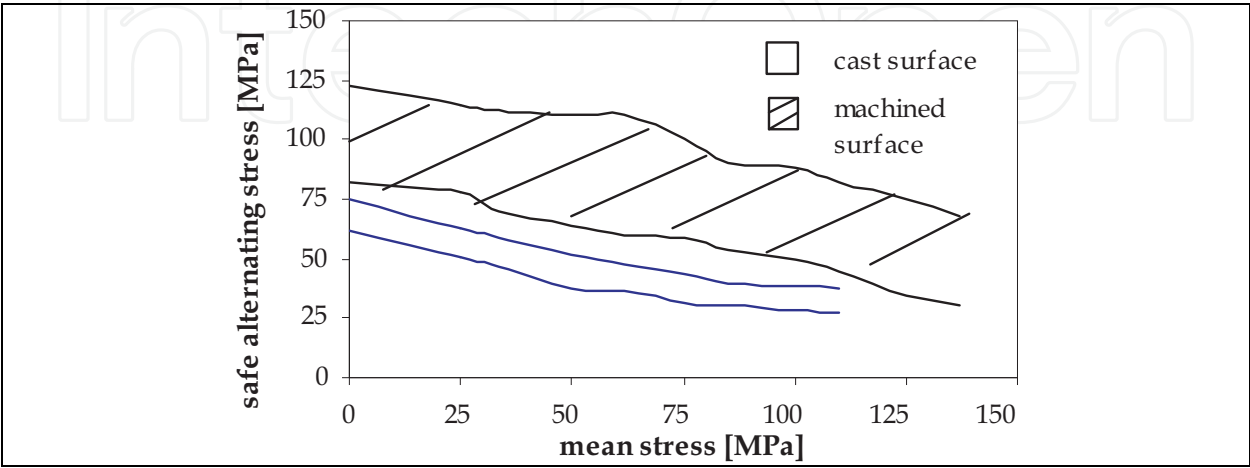


Fig. 2. Influence of the surface quality on the fatigue properties of magnesium alloys

of the microstructure. During the ageing, the homogeneous and inhomogeneous cell structure is created and has influence on the dependence $\sigma_a = f(N)$ (Ishikawa et al., 1997).

When fatigue is the controlling factor in design, every effort should be made to decrease the severity of stress raisers. Use of generous fillets in re-entrant corners and gradual changes of section greatly increase fatigue life. Conditions in which the effects of one stress raiser overlap those of another should be eliminated. Cold working the surfaces of critical regions by rolling or peening to achieve appreciable plastic deformation produces residual compressive surface stress and increases fatigue life. Surface rolling of radii is especially beneficial to fatigue resistance because radii generally are the locations of higher-than-normal stresses.

The initiation of fatigue cracks in magnesium alloys is related to slip in preferable oriented grains and is often related to the existence of micropores. The initial stage of fatigue crack growth usually occurs from quasicleavage, which is common in hexagonal close-packed structures. Further crack growth micromechanisms can be brittle or ductile and trans- or intergranular, depending on metallurgical structure and environmental influence.

On the basis of experimental tests, the authors came to the conclusion that: The dependence fatigue crack growth rate da/dN on the stress intensity factor amplitude ΔK increases with the increasing value of asymmetry coefficient R . The fatigue properties of magnesium alloys decrease with the increasing content of aluminium. Authors (Zheng et al., 2000) observed the influence of loading frequency and heat treatment on the fatigue crack growth rate in magnesium alloy AZ 91HP. The results show that the fatigue crack growth rate in the die-cast magnesium alloy has increased with the frequency decrease. Crack growth can be reduced as a consequence of dissolving annealing or can be increased after ageing. Casting magnesium alloys contain pores filled with air which reduce mechanical properties of the products. Pores have caused the blowholes and deformation during the heat treatment. The studies of fatigue crack growth in magnesium alloy AZ 91D which did not contain pores, have shown two facts. For the low values of ΔK the crack growth is discontinuous and for higher values of ΔK it is continuous. These facts confirm that fatigue crack growth is influenced by heat treatment and environment. It is relationship between growth rate and free surface oxidation. The fatigue crack growth is higher in the air than in argon. The brittle oxidizing film on the free fatigue surface is the cause of it. The ageing increases fatigue crack growth and decreases K_{fc} . However, it shows that ageing does not influence ΔK_{th} ((Ishikawa et al., 1995), (Shibusawa et al., 1997)).

A fundamental study of the corrosion fatigue of magnesium alloys found that both stress-corrosion and corrosion-fatigue cracks propagated in a mixed transgranular - intergranular mode. Corrosion fatigue crack growth is accelerated by the same environments as those that accelerate stress corrosion crack growth. The boundary between regions II and III in sodium bromide solutions of the da/dN versus ΔK curve is higher than the stress corrosion threshold, which occurs at much lower stress intensity.

2.2 Fatigue endurance of magnesium alloys under high frequency cyclic loading

Information about fatigue endurance of magnesium alloys under high frequency cyclic loading is rare. Authors in papers ((Mayer et al., 1997), (Stanzl et al., 1984), (Laird & Charsley, 1982), (Papakyriacou et al., 2001), (Mayer, 1998)) determined fatigue endurance of high pressure die cast magnesium alloys AZ 91HP, AM 60 Hp and AS 21HP under high frequency loading. Fatigue tests of magnesium alloys with chemical composition, shown in tab. 3 were carried out in the air, with temperature $20 \div 22$ °C and warm air with temperature 125°C and final number of cycles was $N = 1.10^9$ cycles.

Mg - alloys	Al	Zn	Mn	Si	Fe	Cu	Ni	Ce
	[wt %]							
AZ 91 HP	8.9	0.79	0.21	0.01	0.003	0.001	0.001	-
AM 60 HP	6.1	0.01	0.29	0.01	0.003	0.002	0.001	-
AS 21 HP	2.2	< 0.01	0.16	0.98	< 0.01	< 0.002	< 0.001	0.073

Table 3. Chemical composition of particular magnesium alloys

Experimental results which were obtained are depicted in Fig. 3 and measured value of fatigue limit σ_c ($N = 1.10^9$ cycles) including fatigue limit σ_c ($N = 1.10^7$ cycles) for particular magnesium alloys are shown in Table. 4. Results of fatigue experiments with AZ 91HP are shown in Fig. 3. Specimens which did not fail are marked with an arrow. Data points for load amplitudes equal or higher than 52 MPa (ambient air, $T = 20 \div 22\text{ }^\circ\text{C}$) and 42 MPa (warm air, $T = 125\text{ }^\circ\text{C}$) are approximated using an exponential function, and the lines indicate a probability for fracture of 50 %. In both environments numbers of cycles to failure greater than about 1.10^7 cycles are rare, and a well defined fatigue limit exists. No specimen failed within 1.10^9 cycles at load levels of 38 MPa (ambient air, $T = 20 \div 22\text{ }^\circ\text{C}$) and 33.5 MPa (warm air, $T = 125\text{ }^\circ\text{C}$), respectively.

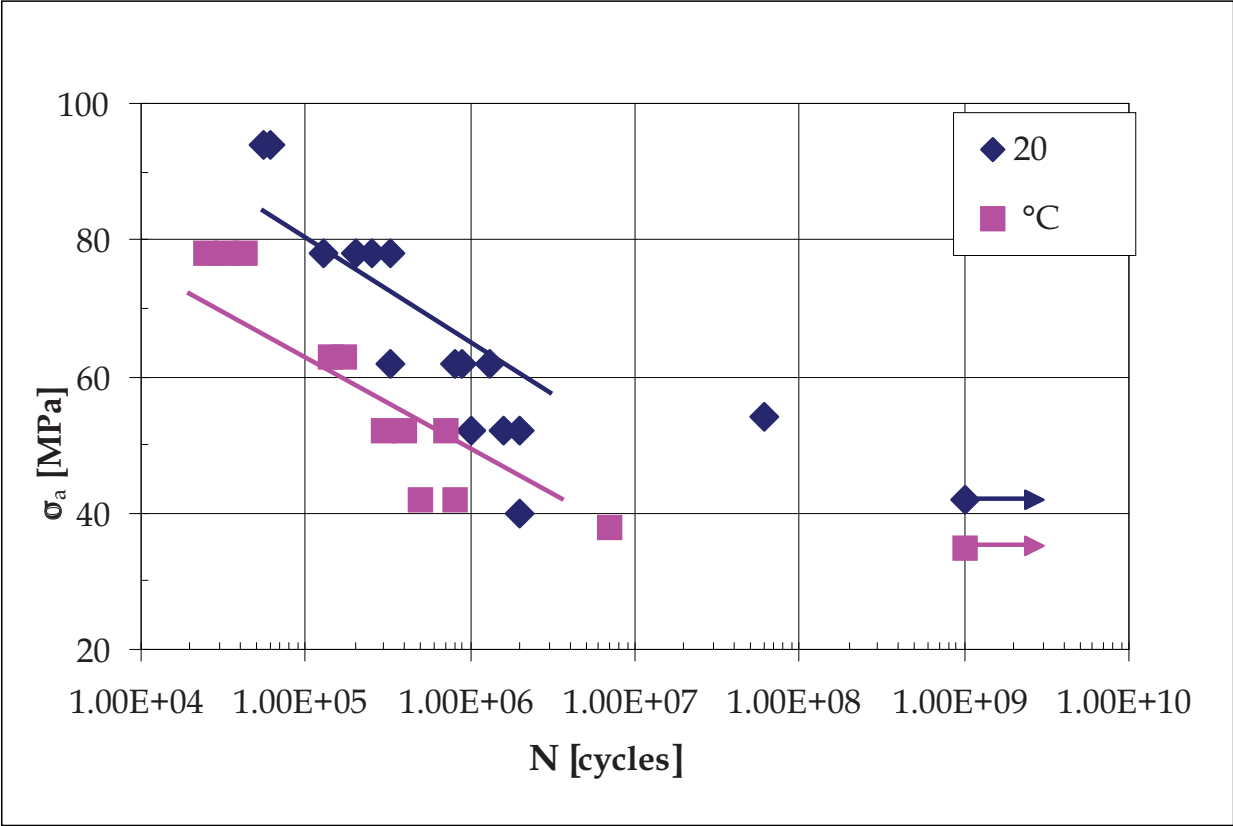


Fig. 3. Dependence $\sigma_a = f(N)$ of magnesium alloy AZ 91HP

A comparison between the S - N curves of AZ 91HP, AM 60HP and AS 21HP is depicted in Fig. 4. In ambient air environment AM 60HP shows longer fatigue life and a higher fatigue limit than AZ 91HP. Fatigue limit in magnesium alloys AZ 91D and AS 21HP is decreasing in approximately 20 % if the temperature increases from $20 \div 22\text{ }^\circ\text{C}$ to $125\text{ }^\circ\text{C}$. Fatigue properties of AS 21HP are worse than those of AZ 91HP and of AM 60HP.

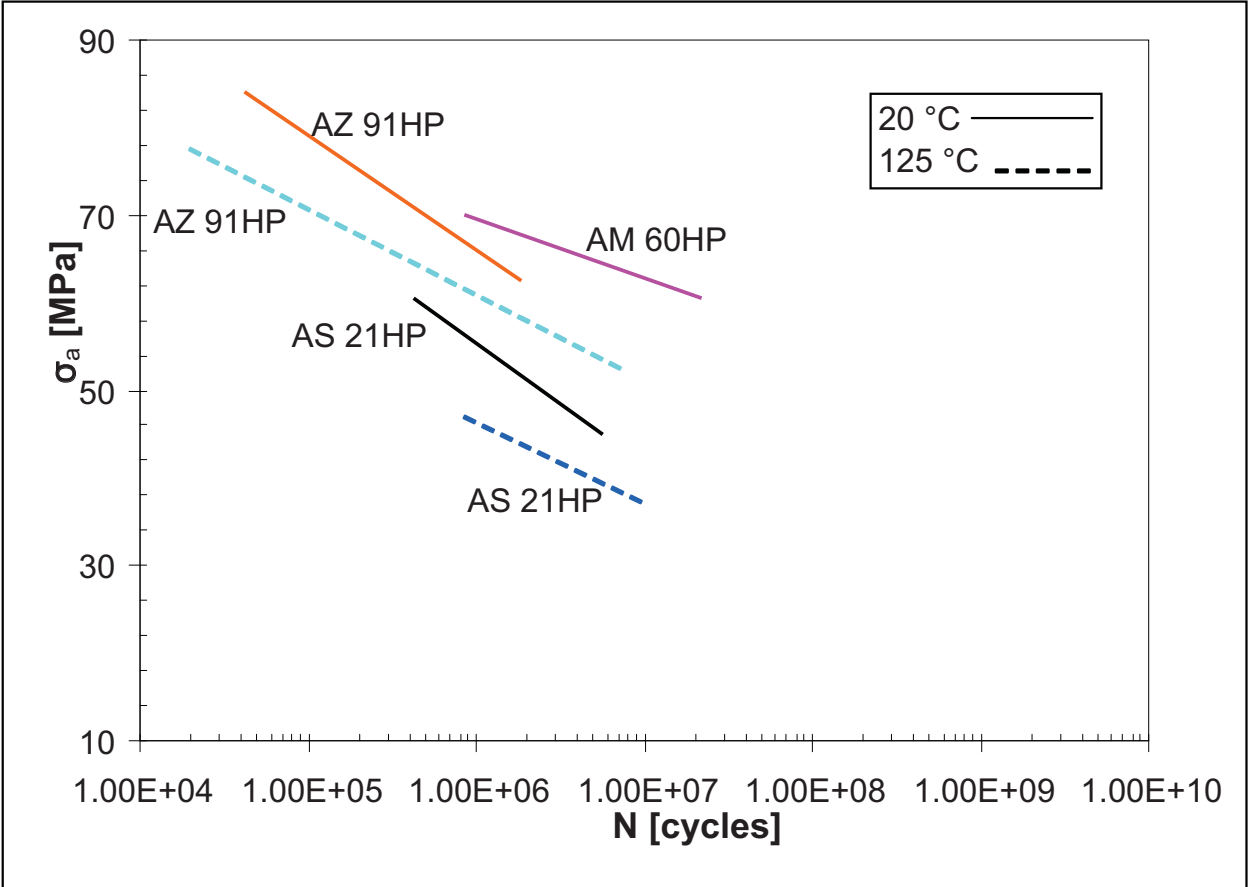


Fig. 4. The comparison of dependence $\sigma_a = f(N)$ of particular magnesium alloys

Fatigue limit		σ_c [MPa]			
Mg - alloy	Number of cycles	N = 1.10 ⁹		N = 1.10 ⁷	
	Temperature	20 °C	125 °C	20 °C	125 °C
AZ 91HP		38	33.5	52	42
AM 60HP		43	-	52	-
AS 21HP		28	21	40	25

Table 4. Fatigue limit σ_c at number of cycles $N = 1.10^7$ and 1.10^9 cycles for particular magnesium alloys

Experimental bars after fatigue tests were undergone a fractographic analysis. Voids were observed on the surfaces of all broken AZ 91HP and AM 60HP specimens, and in crack initiation area on 37 of 40 broken AS 21HP specimens. Fig. 5 shows such a void as an example for that kind of casting defect on the fracture surface of an AZ 91HP specimen which was cycled with load amplitude of 52 MPa and broken after 1.92×10^6 cycles. Some places on the surface of the void show dendrite arms, which indicates that voids are shrinkage, formed during cooling of the melt. Voids serve as starting points for the formation of fatigue cracks. Further crack growth then is transcrystalline in all three investigated materials irrespective of load level and temperature. Voids generally had a very irregular shape and it was sometimes difficult to clearly find the border of that casting defect. In the crack initiation area of some specimens not one but several voids of different size were concentrated.

Subdividing the fatigue process into fatigue crack initiation and crack growth until final failure, voids shorten both fatigue periods. Voids cause stress concentration in nearby material and facilitate crack initiation. Stress amplitude, size, shape and site of a void as well as possibilities for slip in adjacent grains influence the number of cycles to form an initial crack. With increasing size of the casting defects the probability for early crack initiation is increasing (Mayer et al., 1997).



Fig. 5. Void in the fatigue crack initiation area of AZ 91HP under high frequency cyclic loading

An influence of the heat treatment (T6a – dissolving annealing and artificial ageing, T4 – dissolving annealing) on fatigue endurance (dependence $\sigma_{\max} = f(N)$) for magnesium alloy AZ 91D is presented by authors (Ishikawa et al., 2001), and shown in Fig. 6. For both heat treatment the specimens did not fail in the area of number of cycles $N = 1.10^6 \div 1.10^7$ cycles. For that area, magnesium alloy AZ 91D with heat treatment T6a showed better fatigue properties. Authors supposed with respect to the dependence $\sigma_{\max} = f(N)$ that the mechanism of failure was different in dependence on the stress level.

An influence of environment and porosity on fatigue endurance of magnesium alloys was observed in author's work (Mayer et al., 1999). Fatigue experiments were performed in ambient air (temperature $20 \div 22$ °C) and in a saltwater spray (5wt% iodized sodium chloride dissolved in water). Specimens were excited to longitudinal resonance vibrations at ultrasonic frequencies (≈ 20 kHz). The results of fatigue experiments are depicted in Fig. 7. Lines indicated a fracture probability of 50%. In ambient air, failures beyond 1.10^7 cycles were rare and the $S-N$ curve became parallel to the abscissa in the high-cycle regime. Because no specimen failed within 1.10^9 cycles at a stress level of 38 MPa that stress amplitude was defined as the fatigue limit of that material.

In saltwater spray, no significant reduction of fatigue lifetimes, in comparison to ambient air, was found for cycles-to failure below 1.10^7 cycles, and the fatigue date coincided within the range of scatter. For higher numbers of cycles, however, an influence of the corrosive fluid on fatigue properties was observed. The $S-N$ curve decreased in the regime above 1.10^7 cycles, in contrast to the ambient air environment, no fatigue limit was found.

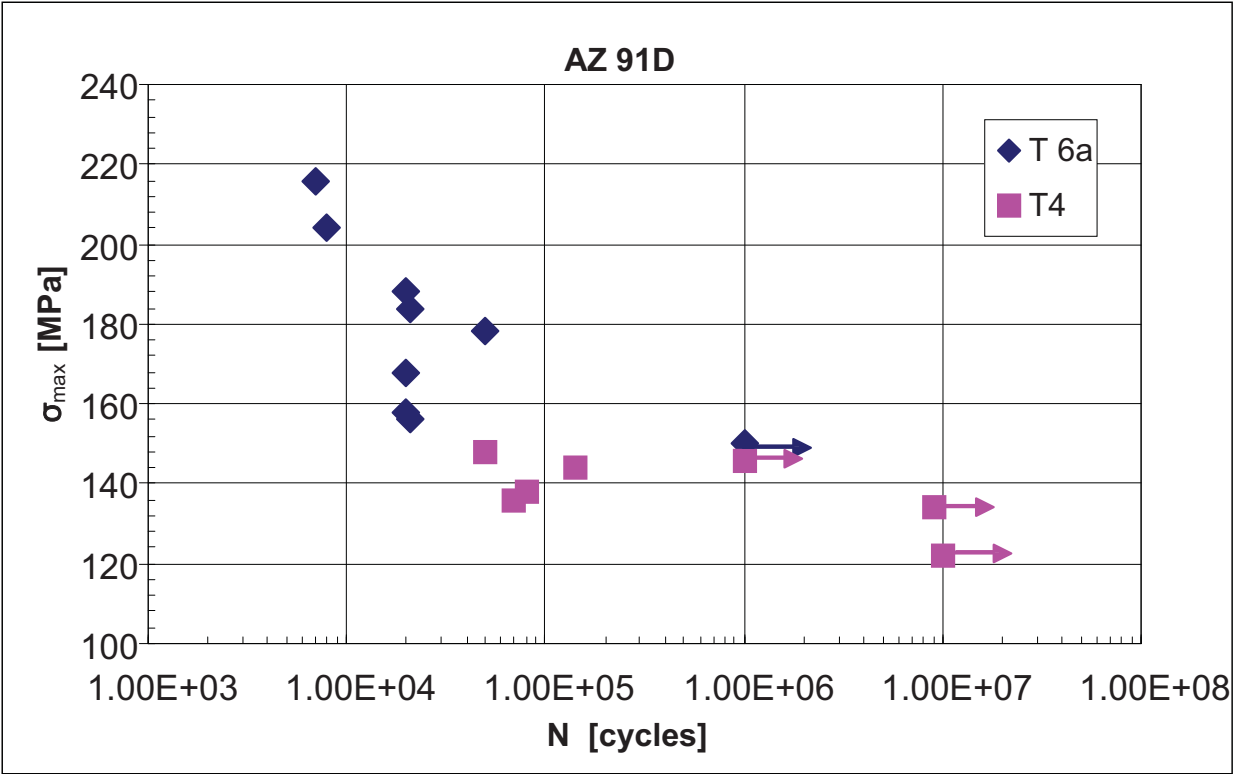


Fig. 6. Dependence $\sigma_{\max} = f(N)$ for magnesium alloy AZ 91D after heat treatment

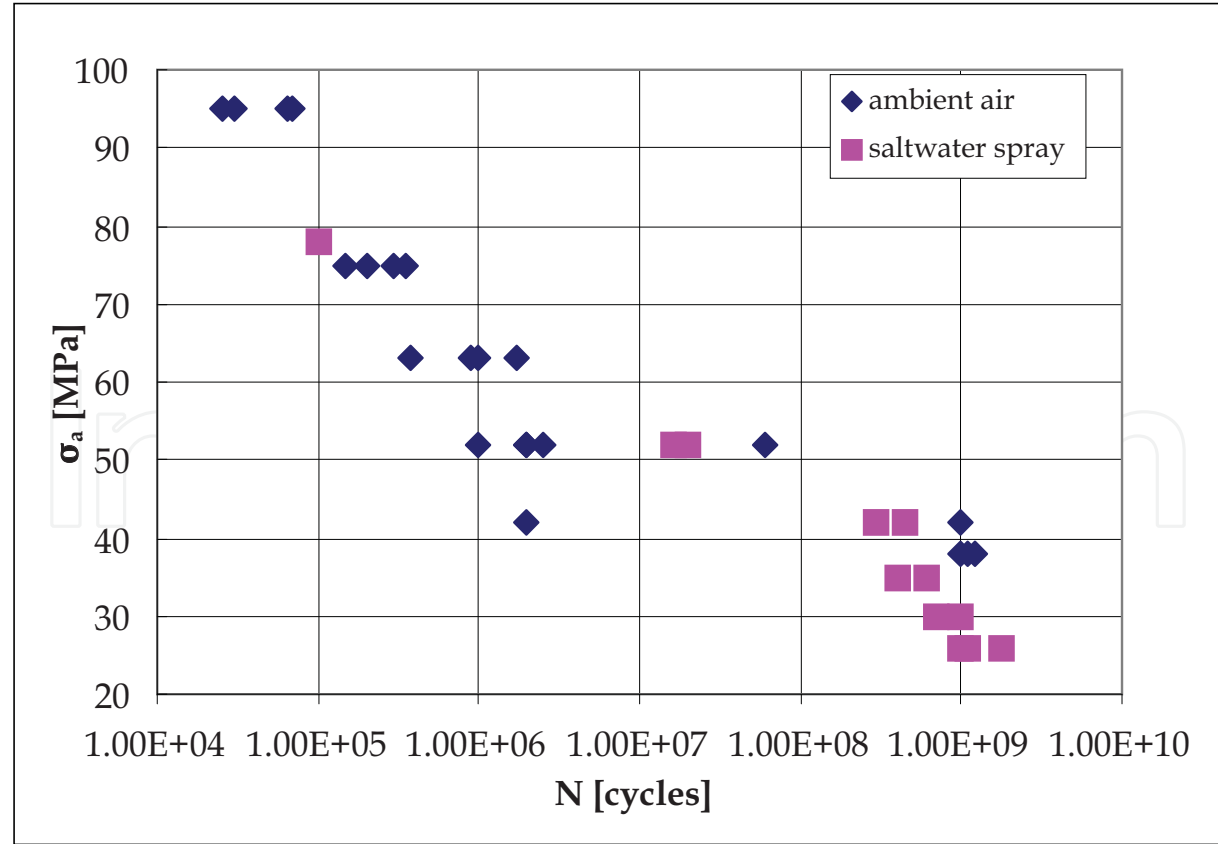


Fig. 7. Results of endurance fatigue tests on AZ 91HP in ambient air at 20 °C and in saltwater spray

If the number of cycles-to-failure was below 1.10^7 , the fracture surfaces of AZ 91HP specimens fatigued in ambient air and saltwater spray were similar. Fatigue cracks emanated from voids in both cases, and the fracture surfaces showed transgranular crack propagation with no significant influence of the corrosive fluid. At very high numbers of cycles-to-failure (1.10^8 and above), cyclic loading in corrosive fluid led to the formation of corrosion pits on the surface of the material. The depth of pits increased approximately linearly with exposure time of the specimen. The lifetime in saltwater spray was not only shorted due to accelerated crack growth, but additionally by the notch effect of those pits which caused local stress concentrations and enabled crack initiation at low applied stress amplitudes. However, AZ 91HP did not show nearly as deep corrosion pits after 42 h corrosion attack if no cyclic loading had been applied. The testing times at ultrasonic frequencies below 1.10^7 ($f = 20$ kHz, $t = 8$ min.) cycles-to-failure probably were too short to lead to a strong corrosive effect in that material. Magnesium alloy AZ 91HP did not show fatigue limit in saltwater spray (Mayer et al., 1999). Ambient air had significant influence on the fatigue crack growth in the threshold regime. Threshold value of stress intensity factor K_{ath} measured in vacuum was $30 \div 85$ % higher than in ambient air. The influence of air humidity decreased at higher fatigue crack growth rates at ultrasonic frequencies. Accelerated fatigue crack growth in magnesium alloys at high growth rates was caused by absorbed hydrogen which had weakened bond between atoms (Lynch, 1988) or hydrogen diffusion which caused embrittlement of material (Makar et al., 1993). A significant reduction in lifetimes was found for sand-cast AZ 91E-T6 when specimens were cycled at conventional frequencies (25 Hz) in saltwater.

The influence of porosity was observed on the fracture surfaces of all AZ 91HP specimens which showed in ambient air that voids were crack initiation points. Most fatigue cracks started at voids on the surface or close to the surface of the specimens, which meant that such flaws were more detrimental than defects in the inner sections of the material. Fatigue crack growth was transcrystalline, irrespective of the load level. Stress concentrations near voids were the source of crack initiation. The increase of the nominal stress in the remaining cross-section was limited. Because a larger initially broken area caused higher cyclic stress intensity amplitude, the crack growth period at a certain cyclic load was shorter for larger flaws. Most fractured specimens failed below $1 \div 2.10^7$ cycles, and the $S-N$ curve at higher number of cycles was approximately parallel to the abscissa. The rather low fatigue limit of AZ 91HP was attributed to the manufacturing process leading to relatively large casting voids and it was not an inherent property of that magnesium cast alloy. Fatigue tests of magnesium alloy AZ 91HP produces with different casting techniques showed that the $S-N$ curve determined permanent mould-casted AZ 91HP material without voids lain above the $S-N$ of die-cast AZ 91HP, however, it decreased in the entire investigated regime between $1.10^5 \div 1.10^9$ cycles and did not show a fatigue limit. In cases where specimens failed after more than 1.10^7 cycles, cracks emanated from voids in the inner section of the material. It meant that fatigue cracks grew mainly under vacuum conditions.

3. Fatigue endurance of magnesium alloys AZ 91D and AZ 63HP

3.1 Experimental materials

Fatigue experiments were performed with the sand-cast magnesium alloys AZ 91D and AZ 63 HP after heat treatment T4 – dissolving annealing according to Fig. 8. AZ 91D is the most frequently using alloy, mostly in automobile industry. AZ 63 HP is alloy with high purity and reduced content of copper, ferrum and silicon.

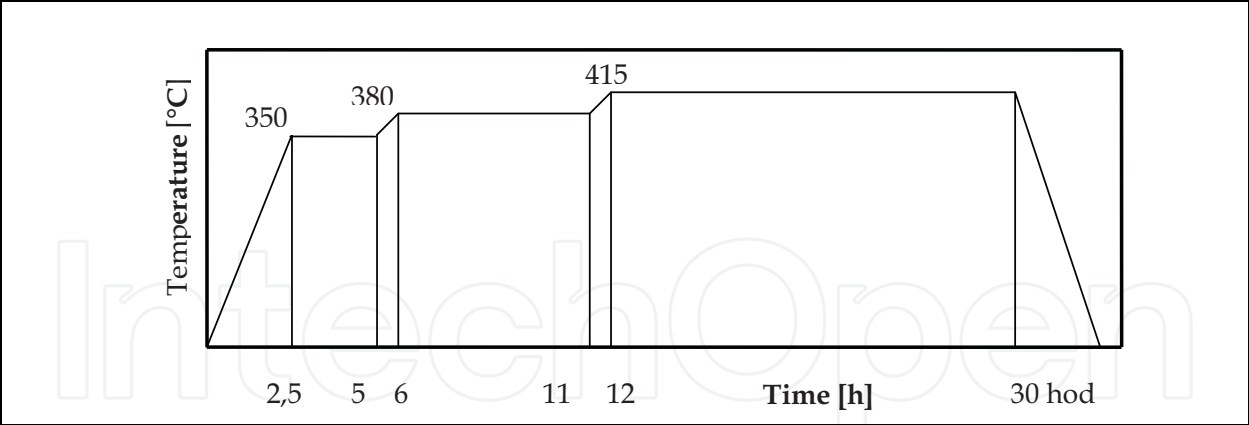


Fig. 8. Heat treatment regime of magnesium alloys AZ 91 and AZ 63HP

Magnesium alloys were delivered after being cast into sand moulds in the form of half-finished products, i.e. plates with dimensions 21 x 100 x 200 mm (Fig. 9a) and blocks with dimensions 70 x 160 x 160 mm (Fig. 9b). Due to non-uniform hardening in the course of experimental material cooling, specimens were taken from the block and the plate edge as well as the plate middle (Fig. 9).

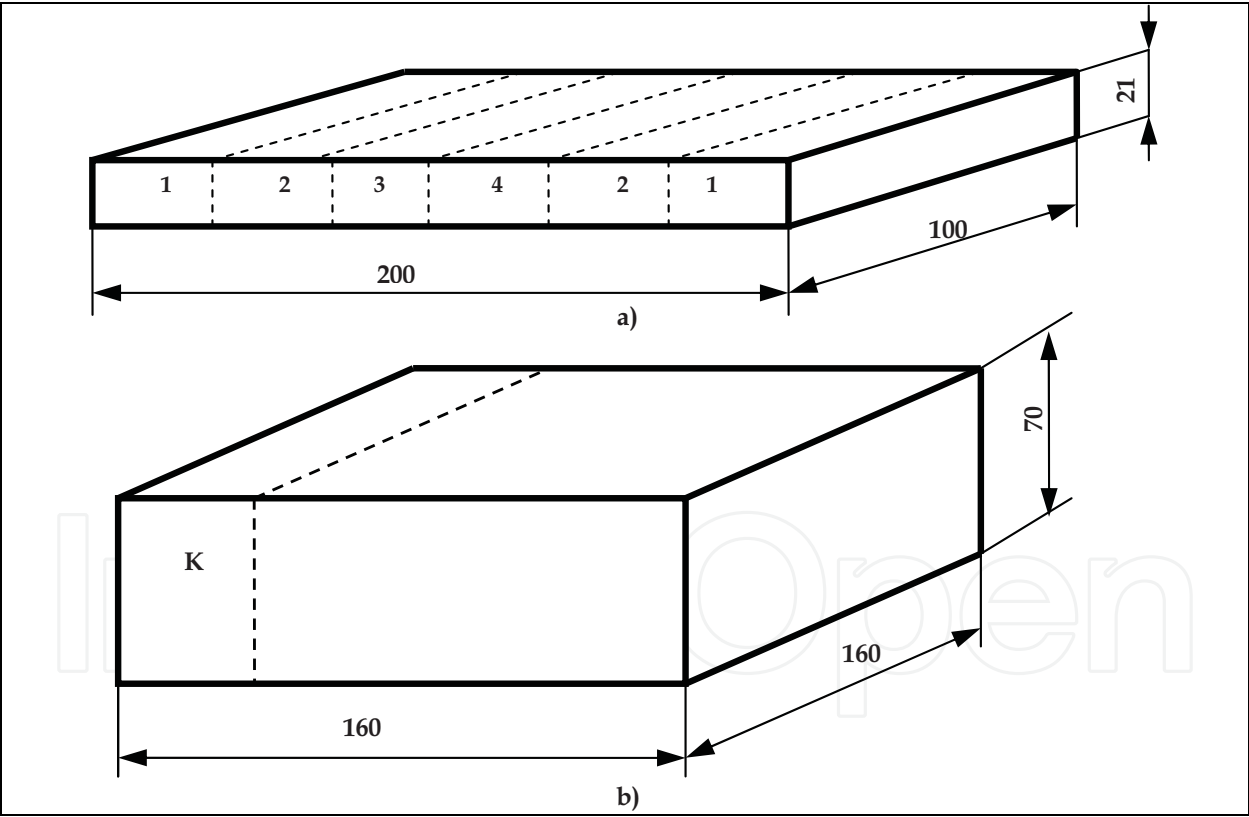


Fig. 9. Taking, marking and using of specimens, a – plate, b – block

- 1, 2 – fatigue test, metallographic analysis, Brinell hardness test, tensile test
– marked **plate edge**
- 3, 4 – fatigue test, metallographic analysis, Brinell hardness test
– marked **plate middle**
- K – fatigue test, metallographic analysis, Brinell hardness test, falling-weight test
– marked **block**

Chemical composition and mechanical properties of magnesium alloys AZ 91D and AZ 63HP are shown in Tab. 5, Tab. 6 and Tab. 7.

Mg-alloy	Al	Zn	Mn	Si	Cu	Fe	Be	Pb
AZ 91D	7.98	0.63	0.22	0.045	0.007	0.013	0.0003	0.057
AZ 63HP	5.28	2.65	0.21	0.028	0.002	0.003	0.0003	0.037

Tab. 5. Chemical composition (wt %) of magnesium alloys AZ 91D and AZ 63HP

Mg- alloy	Rm [MPa]	Re [MPa]	A ₅ [%]	Z [%]	KCU 2 [Jcm ⁻²]
AZ 91D	223	76	8	0.5	4.4
AZ 63HP	121	59	6.2	0.3	6.6

Tab. 6. Mechanical properties of magnesium alloys AZ 91D and AZ 63HP

Mg - alloy	Plate edge	Plate middle	Block
AZ 91D	64.2	65.5	67.5
AZ 63HP	63.6	63.0	60.6

Tab. 7. Value of Brinell hardness test, HB_{2.5/62.5/30} for magnesium alloys AZ 91D and AZ 63HP

Microstructure of magnesium alloy AZ 91D specimens after heat treatment (Fig. 8) is presented in Fig. 10. Specimens for metallographic analysis were taken from block, plate edge as well as plate middle. Microstructure of the specimens taken from the block (Fig. 10a) was the complicated heterogeneous structure which was extremely influenced by the cooling rate and therefore the microstructure after heat treatment was considerably influenced by microstructure of half-finished product. The structure was created by non-uniform large dendritic grains of phase δ (grain size 2) and discontinuous eutectic ($\gamma + \delta$) precipitated on the grain boundaries. The eutectic was created by fine lamellas of phase γ (electron compound $Al_{12}Mg_{17}$) with huge number of voids (black points). Phase γ was in attendance in the form of primary precipitated massive phase (precipitated on the dendrite boundaries) which was surrounded by the eutectic. Presence of the voids was characteristic for the whole structure. Microstructure of the specimens taken from the plate with the thickness 21 mm (Fig. 10b, c) was created by polyedric grains of phase δ . The grain size was not the same in the whole cast body. Bigger grain was observed in specimens taken from the plate middle (grain size 4) (Fig. 10b) when compared to the specimens taken from the plate edge (grain size 5) (Fig. 10c). At some places, within the grain boundaries there was found the presence of small amount of discontinuous precipitate consisting of fine lamellas of phase γ (electron compound $Al_{12}Mg_{17}$) in matrix of δ phase. In that case, there were observed the characteristic meandering grain boundaries with the rest of lamellar precipitate (Fig. 12a).

Character of the microstructure of magnesium alloy AZ 63HP was mainly given by different chemical composition (lower content of Al, higher content of Zn). As a consequence, the microstructure was mostly characterized by phase δ and small amount of the precipitate. Microstructure of the specimens taken from the block (Fig. 11a) was created by non-uniform polyedric phase δ (grain size 1 - 2) with the areas of lamellar precipitate on the grain boundaries. Black places presented the presence of voids. Microstructure of the specimens

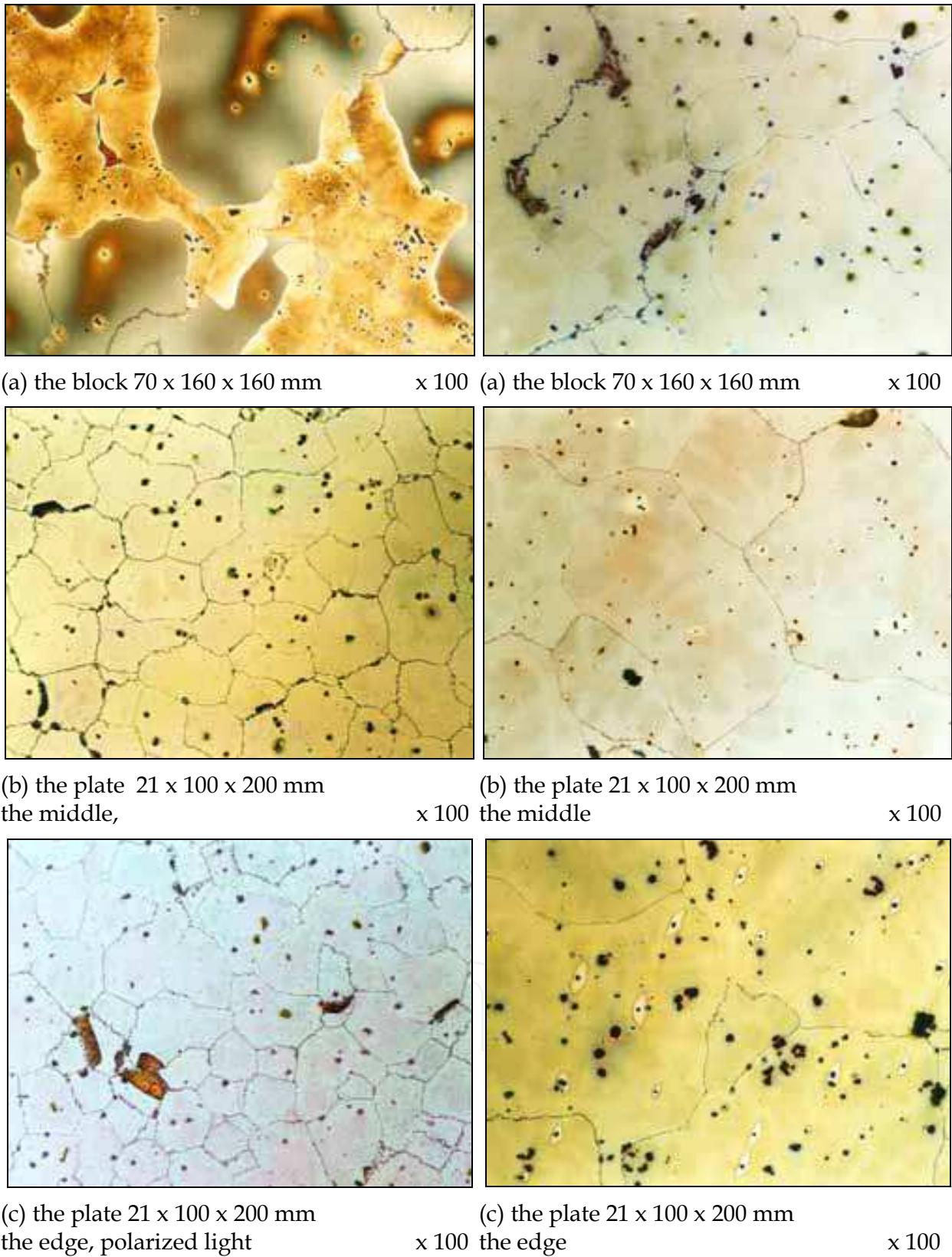
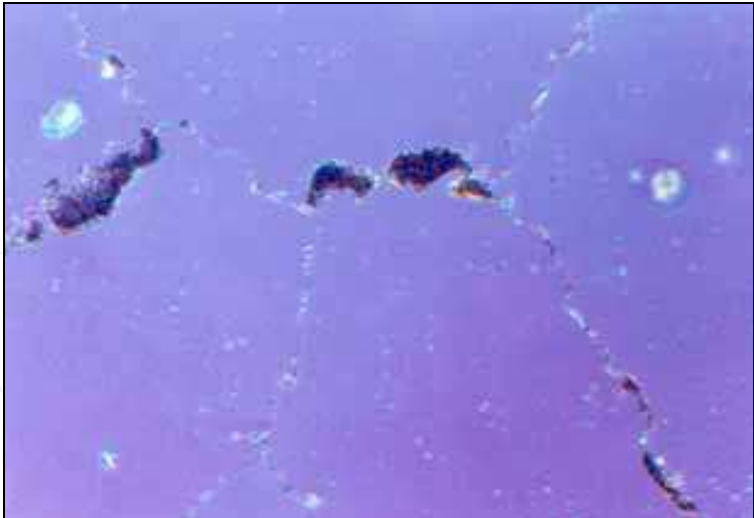


Fig. 10. Microstructure of magnesium alloy AZ 91D after heat treatment T 4, etch. 5 % molybdenum acid

Fig. 11. Microstructure of magnesium alloy AZ 63HP after heat treatment T 4, etch. 5 % molybdenum acid



(a) Mg – alloy AZ 91D, the plate middle x 500



(b) Mg – alloy AZ 63HP, the plate edge, the lamellar precipitate x 500



(c) Mg – alloy AZ 63HP, the plate middle, the meandering boundaries x 500

Fig. 12. Details of microstructure of Mg – alloys AZ 91D and AZ 63HP after heat treatment T4, etch. 5 % molybdenum acid, polarized light

taken from the plate was analogical (Fig. 11b, c). The presence of lamellar precipitate was sporadically observed in the specimens taken from the plate middle (Fig. 11b). Detail of the lamellar precipitate is shown in Fig. 12b. There were observed the characteristic meandering grain boundaries of phase δ (grain size 1) with the rest of the precipitate. The presence of lamellar precipitate (Fig. 11c) was not identified in the structure of the specimens taken from the plate edge (grain size 2 - 3). The grain boundaries were markedly meandering and the rest of the lamellar precipitate (Fig. 12c) was observed on the grain boundaries.

Assessment of the individual effects of particular types of precipitate morphologies on the properties of the material is difficult as all of them exist in the same material. Generally these kind of cellular microstructures are considered as detrimental to the toughness of the material. When evaluating the effect of discontinuous precipitation on mechanical properties the nodule size should also be considered. Elimination of this type of precipitation reaction in Mg based alloys would be desirable as it is also claimed to accelerate creep at high temperatures. Furthermore, this would allow for more extensive continuous precipitation leading to better strengthening effect. Coarse γ particles at the grain boundaries are the product of a divorced eutectic reaction from the Al enrich part of the liquid metal that solidifies the last in a casting. The continuous precipitation products in AZ 91 are known to nucleate on dislocations, twin boundaries and interiors. Slower cooling rates increase the amount of discontinuous precipitation (Kaya et al., 2000).

3.2 Experimental fatigue tests of magnesium alloys AZ 91D and AZ 63HP

The testing bars using in experimental works were designed to be in accord with recommendations ((Salama & Lamerand, 1982), (Puškár et al., 1987)) to follow the resonance conditions. Testing bars for the observation of the dependence $\sigma_a = f(N)$ which shape and dimensions are depicted in Fig. 13, were in the middle, the working area softly ground and polished in order to eliminate the surface influence on the fatigue properties. They were made from the specimens taken from the plate edge and plate middle (Fig. 9a) as well as from the block (Fig. 9b). Testing bars for fatigue crack growth observation, Fig. 14, had a flat shape with the ground and polished surface in the working area and in the middle of it was made artificial notch with the diameter 1 mm as a stress concentrator for fatigue crack growth. They were made from specimens taken from the plate middle.

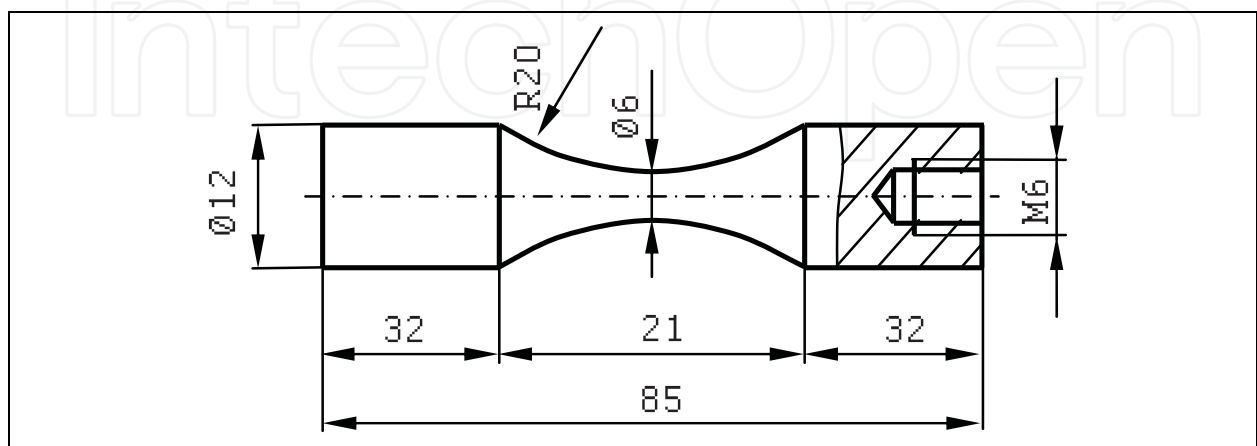


Fig. 13. Shape and dimension of bars using to determination of dependence $\sigma_a = f(N)$, HFCL

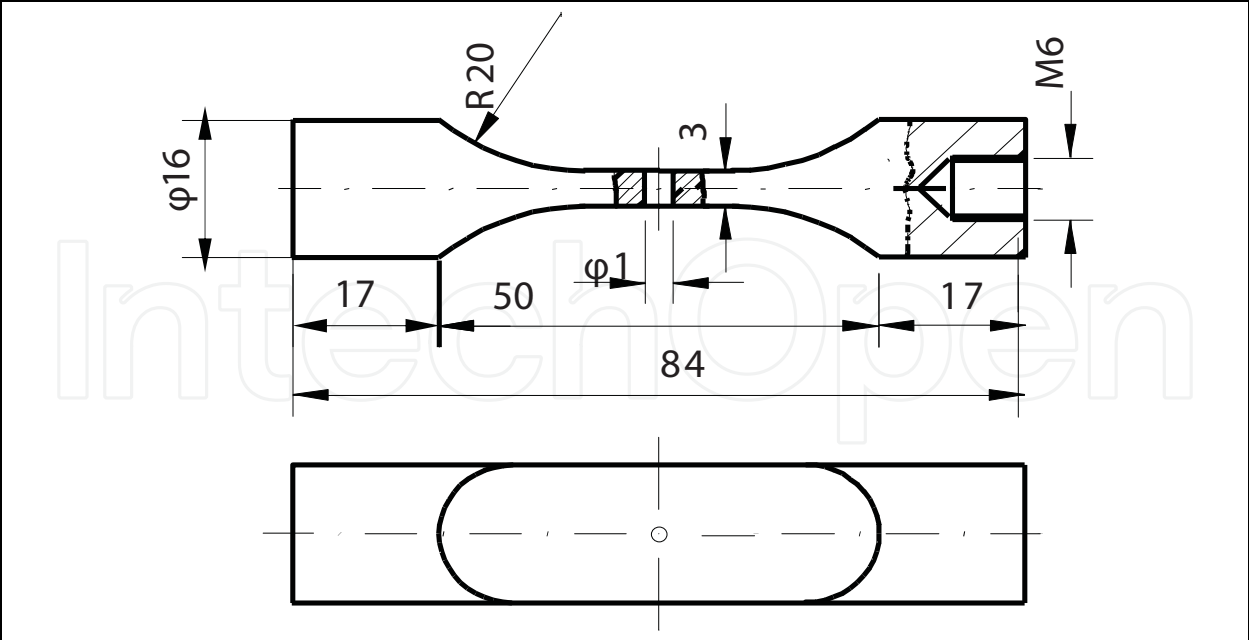


Fig. 14. Shape and dimension of bars using to determination of the dependence $da/dN = f(K_a)$, HFCL

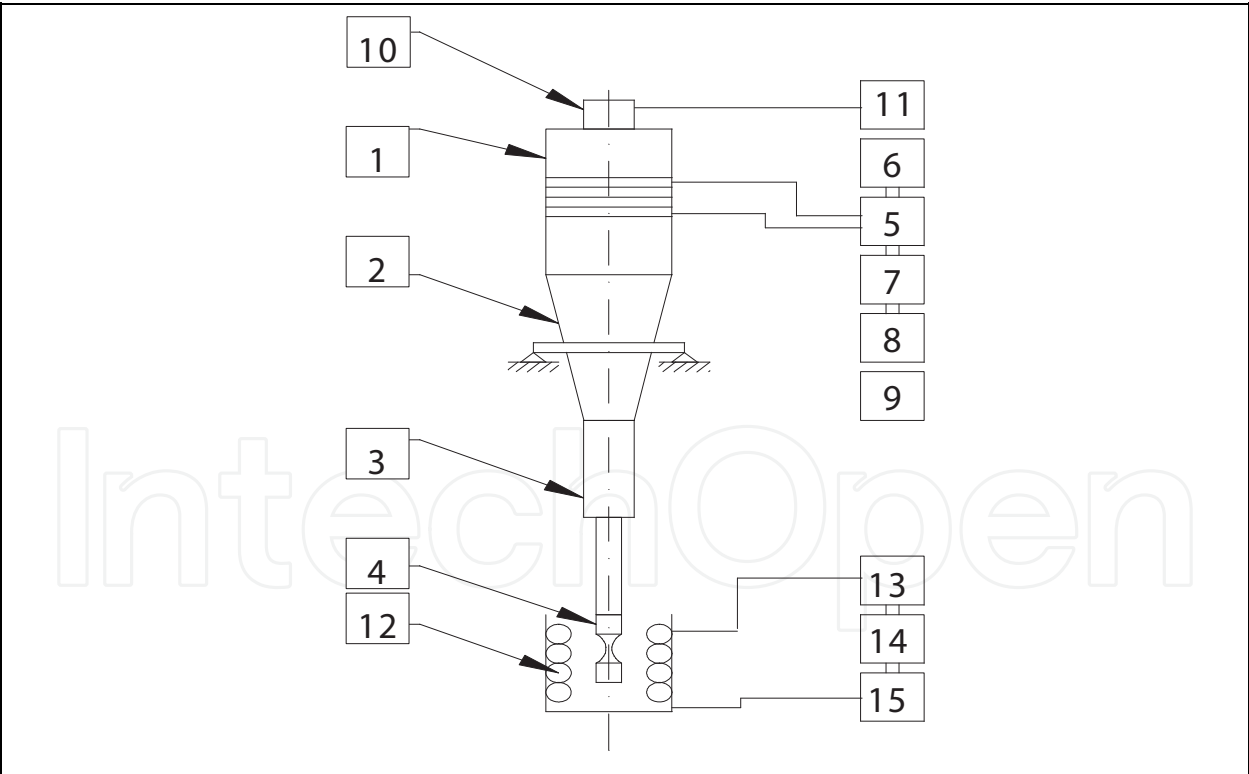


Fig. 15. Schematic device CAFS, HFCL (Puškár, 1997),
(1)- piezoelectric transducer, (2) - conical concentrator, (3) - stepped concentrator, (4) - testing bar,
(5) - ultrasonic generator, (6) - automatic frequency balancer, (7) - frequency meter, (8) - printer,
(9) - stop watch, (10) - sensor of amplitude displacement, (11) - milivoltmeter, (12) - cooling solution,
(13) - thermostat, (14) - water pump, (15) - header.

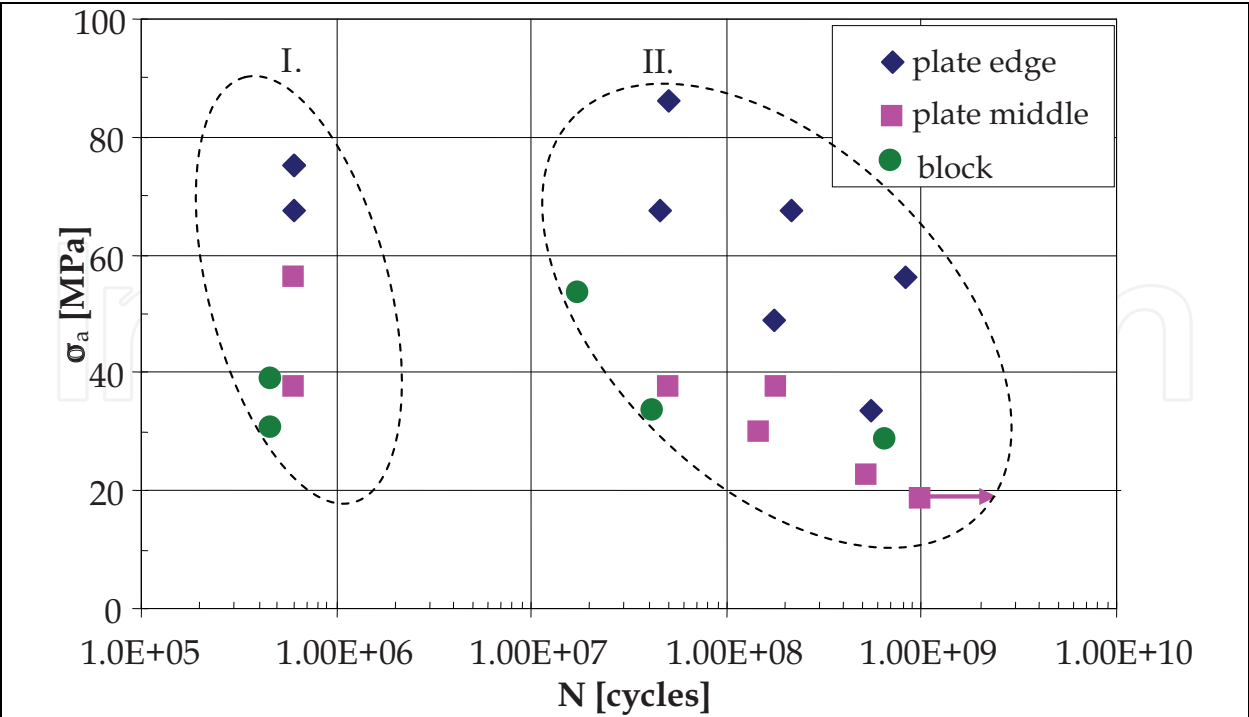


Fig. 16. Experimentally obtained dependences $\sigma_a = f(N)$ for magnesium alloy AZ 91D, HFCL

Fatigue tests were carried out on the experimental device CAFS (Complex Acoustic Fatigue Strength) (Fig. 15) under the high frequency cyclic loading in the very high- cycle regime ($N = 1.10^9$ cycles) using the high frequency resonance method. Using that method, bars were excited to longitudinal resonance vibrations at ultrasonic frequencies (≈ 20 kHz). That led to sinusoidal cyclic loading with maximum load amplitude in the centre of the bar. The fatigue experiments were performed with constant cyclic loads and no static preload was superimposed, load ratio $R = -1$. An amplitude control unit guaranteed that the prestated and the actual displacement amplitudes agreed within 99 % during experiments. Because crack growth increased the compliance of the bars and reduced the resonance frequency, control of the loading frequency was necessary. The bars were cycled until they failed or up to $N = 1.10^9$ cycles if they did not fail (marked by arrow).

Fatigue experiments were performed in ambient air, temperature $20 \pm 10^\circ\text{C}$. During the test the bar was cooling in solution of NaOH.

The obtained results of experimental measurements are depicted in Fig. 16 for magnesium alloy AZ 91D and in Fig. 17 for magnesium alloy AZ 63HP.

Shape of the dependence $\sigma_a = f(N)$ for the testing bars made from the specimens taken from the plate edge was observed in the range $N = 6.10^5 \div 1.10^9$ cycles. Bars which did not fail are marked with an arrow. From the Fig. 16, it is obvious that the stress amplitude σ_a decreases with the increasing number of loading cycles within the range. The stress amplitude σ_a is 75 MPa for $N = 6.10^5$ cycles and $\sigma_a = 56$ MPa for $N = 8.10^8$ cycles. A difference of the stress amplitudes is conceived $\Delta \sigma_a = 19$ MPa. Similar shape of the dependence is observed for testing bars taken from the plate middle. The decrease of stress amplitude σ_a with the increasing number of cycles-to-failure is evident from the Fig. 16 ($\sigma_a = 56$ MPa for $N = 6.10^5$ cycles, $\sigma_a = 18$ MPa for $N = 1.10^9$ cycles, the difference of the stress amplitudes is $\Delta \sigma_a = 38$ MPa). Because no bars failed within 1.10^9 cycles at a stress level of 18 MPa, this stress amplitude is defined as a fatigue limit of this material. For this experimental material, Mg -

alloy AZ 91D the considerable scatter of results of number of cycles N at the particular stress levels σ_a is characteristic. The dependence $\sigma_a = f(N)$ for testing bars taken from the block has slightly declining character (nearly parallel to the coordinates of number of cycles). The stress amplitude σ_a is 38 MPa for $N = 5 \cdot 10^5$ cycles and σ_a is 30 MPa for $N = 7 \cdot 10^8$ cycles. The difference of the stress amplitudes is $\Delta \sigma_a = 8$ MPa. The results are considerably influenced by the place of bars taking.

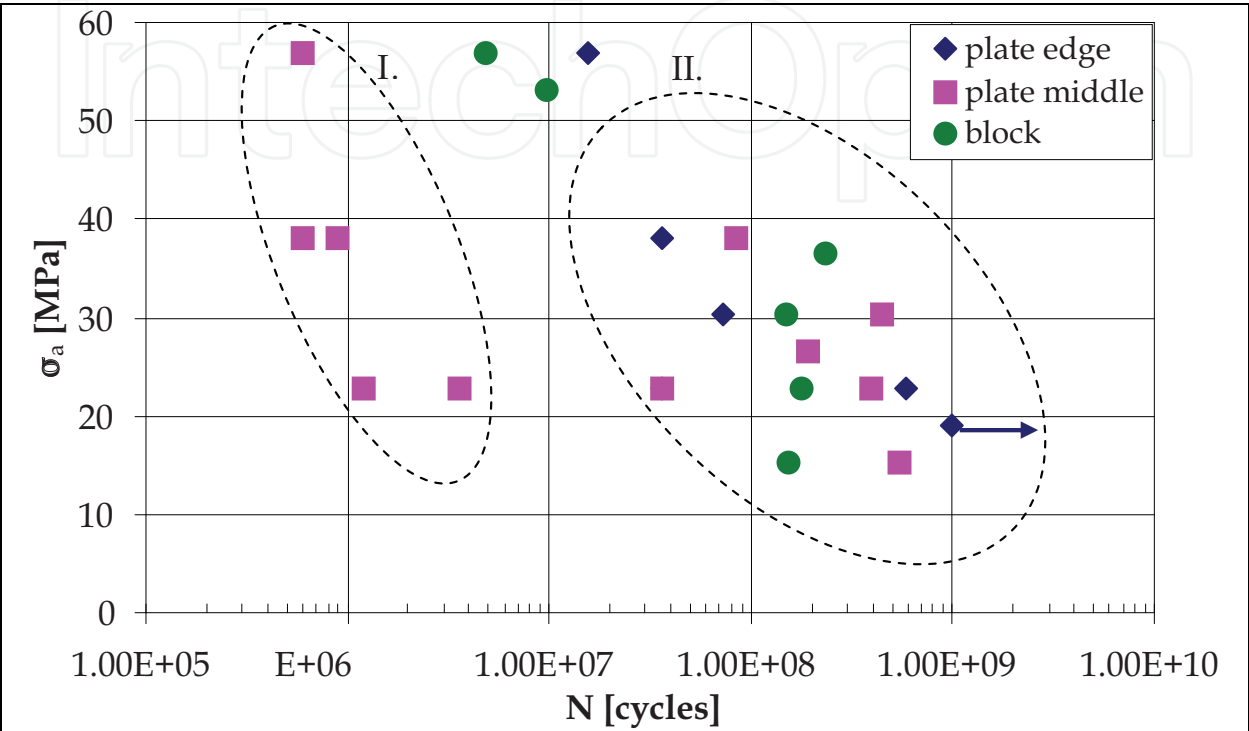


Fig. 17. Experimentally obtained dependences $\sigma_a = f(N)$ for magnesium alloy AZ 63HP, HFCL

The scatter of results of magnesium alloy AZ 63HP (Fig. 17) depended on the place of the bars taking is not as substantial as for the alloy AZ 91D. The shape of the dependence $\sigma_a = f(N)$ for testing bars made from the specimens taken from the plate edge has a decreasing character within the range $N = 1.8 \cdot 10^7$ cycles to $N = 1.1 \cdot 10^9$ cycles. The difference of amplitude $\Delta \sigma_a = 39$ MPa ($\sigma_a = 57$ MPa for $N = 1.56 \cdot 10^7$ cycles and $\sigma_a = 18$ MPa for $N = 1.1 \cdot 10^9$ cycles). The scatter on one stress level is small – one order. After $N = 1.1 \cdot 10^9$ cycles testing bar at the stress level $\sigma_a = 18$ MPa did not fail and it is considered as the fatigue limit. Decreasing shape of dependence $\sigma_a = f(N)$ was observed for testing bars made from the specimens taken from the plate middle as well. Decrease of the stress amplitude has slight character ($\sigma_a = 57$ MPa for $N = 6 \cdot 10^5$ cycles and $\sigma_a = 15$ MPa for $N = 5 \cdot 10^8$ cycles). The difference of amplitude $\Delta \sigma_a = 42$ MPa. For the testing bars made from the specimens taken from the block was observed the most considerable decrease within the range $N = 4 \cdot 10^6$ to $N = 2 \cdot 10^8$ cycles. The difference of amplitude $\Delta \sigma_a = 42$ MPa ($\sigma_a = 57$ MPa for $N = 4 \cdot 10^6$ cycles and $\sigma_a = 15$ MPa for $N = 1 \cdot 10^8$ cycles)

For the magnesium alloys AZ 91D and AZ 63HP, the fatigue crack growth was observed on the testing bars (Fig. 14). The testing bar was initially excited by stress amplitude σ_a , in which the crack started growing. The stress amplitude was decreased gradually unless the crack stopped without failure. Those cycled bars were observed by a light microscope (Fig. 18, 19) and an electron microscope (Fig. 20, 21).

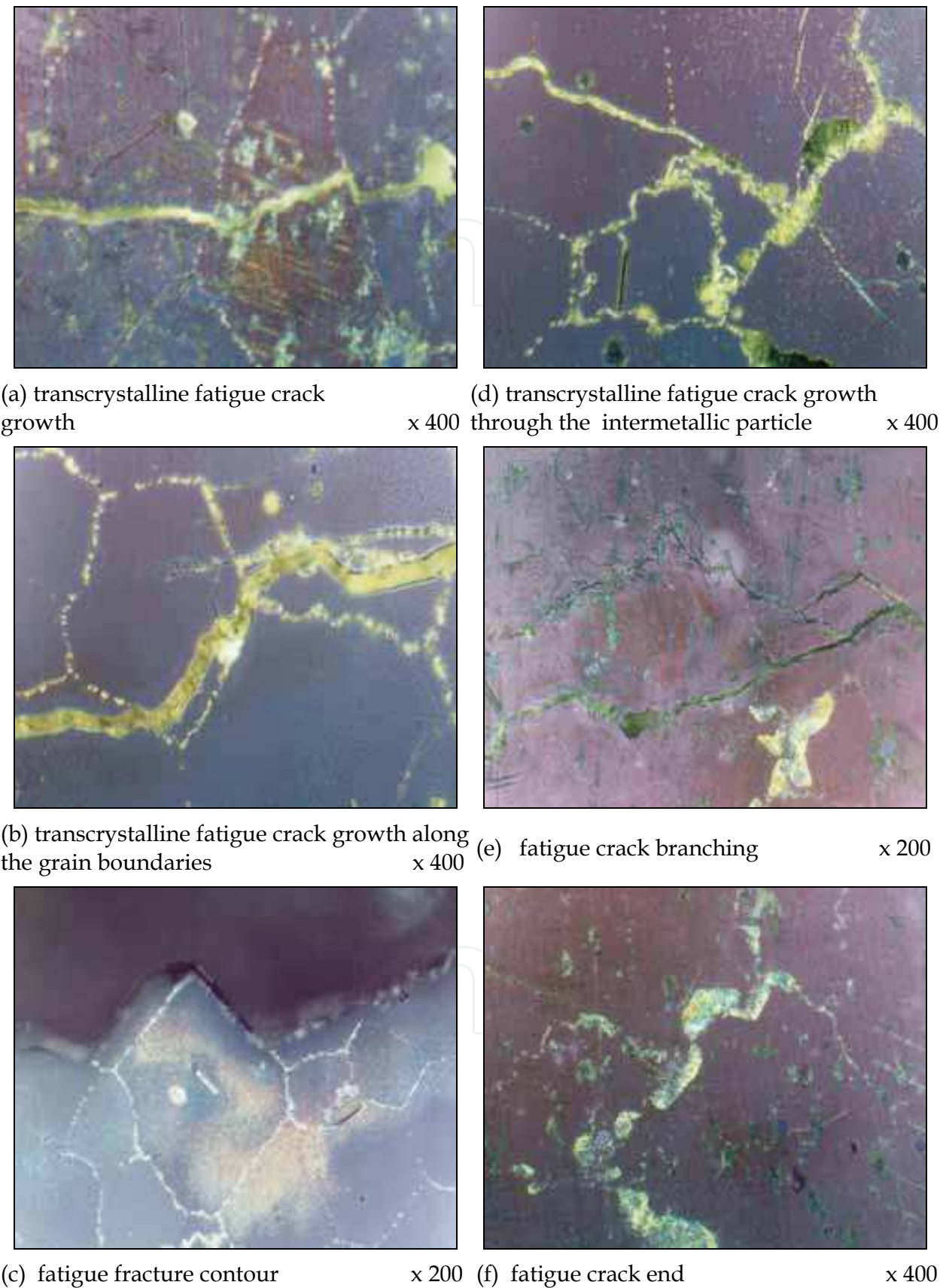
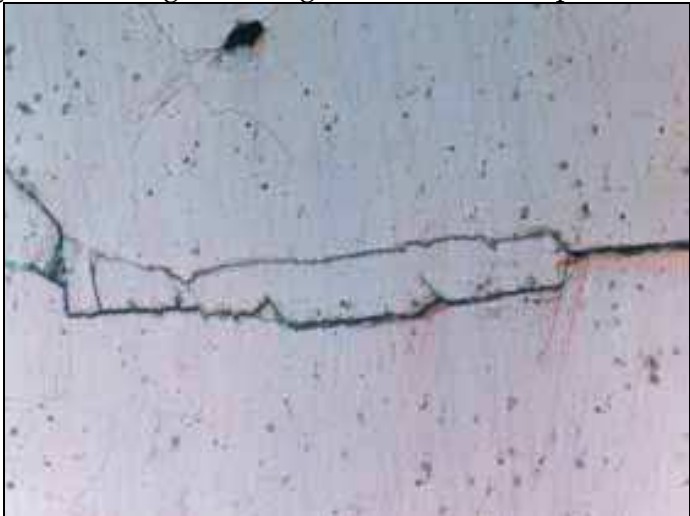


Fig. 18. Fatigue crack growth in magnesium alloy AZ 91D, light microscopy



a) transcrystalline fatigue crack growth with the slip bands x 400



b) fatigue crack branching x 100



c) fatigue fracture contour x 200

Fig. 19. Fatigue crack growth in magnesium alloy AZ 63HP, light microscopy

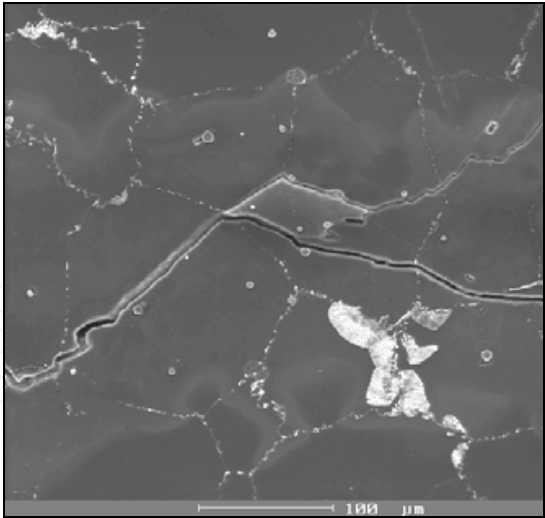
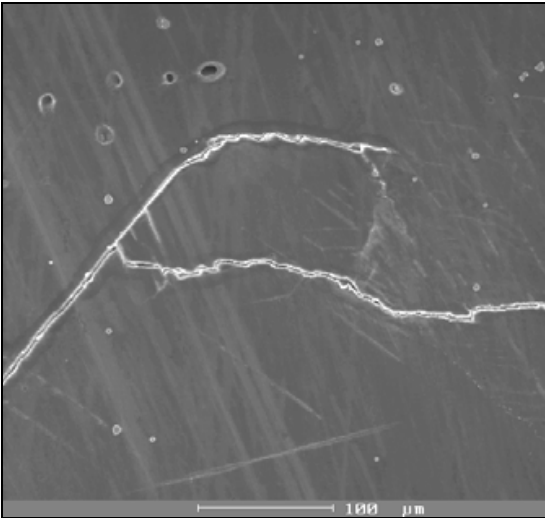
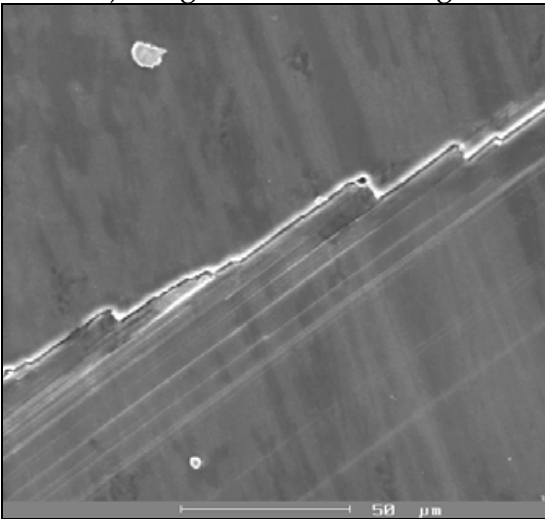


Fig. 20. Fatigue crack growth trajectory in Mg – alloy AZ 91D, S.E.M.



a) fatigue crack branching



b) steps with slip bands

Fig. 21. Fatigue crack growth trajectory in Mg-alloy AZ 63HP, S.E.M.

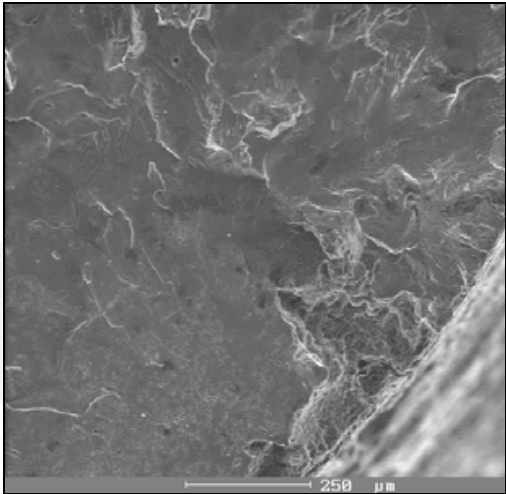
The main fatigue crack grew in magnesium alloy AZ 91D transcrystallically (Fig. 18a, 19a) despite the lamellar precipitate and rest of lamellar eutectic precipitated on the grain boundaries. At higher value of stress intensity factor K_a the fatigue crack trajectory was less dissected and propagation of fatigue cracks was accompanied by intensive slip what was proved by slip bands in the vicinity of the fatigue crack (Fig. 18a). With gradually decreasing value of stress intensity factor K_a the trajectory of fatigue cracks became more dissected and the propagating crack started to copy their boundaries in their vicinity in some of the grains (Fig. 18b). Sporadically there was observed also intercrystalline crack growth (Fig. 18c, 20) as a consequence of weakening of grain boundaries by precipitate or eutectic. When the fatigue crack grew through the intermetallic particles those particles were damaged by brittle failure and the fatigue crack did not change its direction (Fig. 18d). At near-threshold values of stress intensity factor, there occurred branching of cracks as well as an extensive network of secondary cracks (Fig. 18e). When the fatigue crack reached the threshold value of stress intensity factor K_{ath} the fatigue crack growth was stopped (Fig. 18f). The main fatigue crack in the magnesium alloy AZ 63HP propagated transcrystallically and its growth was accompanied by slip with the intensive slip bands in its vicinity (Fig. 19a). At lower value of stress intensity factor K_a , there occurred crack branching (Fig. 19b) and formation of secondary ineffective cracks (Fig. 21a). There were observed the steps (Fig. 19c), during the fatigue crack growth, which presence was accompanied by characteristic slip bands orientated perpendicularly to fatigue crack growth direction (Fig. 21b). The main crack stopped as soon as reached threshold value of stress intensity factor K_{ath} .

The fractographic analysis was performed on the testing bars after fatigue tests. There were observed the fracture surfaces of particular testing bars at low stress levels σ_a in the area of number of cycles $N = 3.6 \times 10^7$ to $N = 6.61 \times 10^8$ cycles. As it was proved by metalographic analysis, final structure was considerably influenced by place of specimen's taking. Variety of structure as well as scatter of results at the same stress levels σ_a was showed during fatigue tests as well as by fractographic analysis.

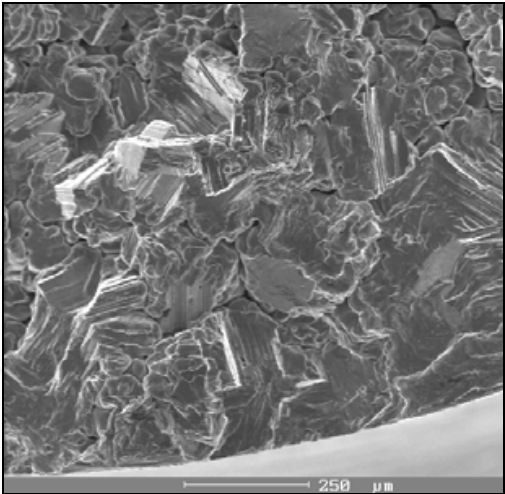
In magnesium alloy AZ 91D, there were observed testing bars broken at stress level $\sigma_a = 30$ MPa. Number of cycles-to-failure at that stress level was $N = 5.57 \times 10^8$ cycles (testing bar made from specimen taken from the plate edge), $N = 1.8 \times 10^8$ cycles (testing bar made from specimen taken from the plate testing bar made from specimen taken from the plate middle) and $N = 6.61 \times 10^8$ cycles (testing bar made from specimen taken from the block).

Observed testing bars of magnesium alloy AZ 63HP were broken at the stress level $\sigma_a = 22.8$ MPa. Number of cycles-to-failure was for particular bars followed: $N = 3.6 \times 10^7$ cycles (testing bar made from specimen taken from the plate edge), $N = 3.65 \times 10^7$ cycles (testing bar made from specimen taken from the plate middle) and $N = 1.78 \times 10^8$ cycles (testing bar made from specimen taken from the block).

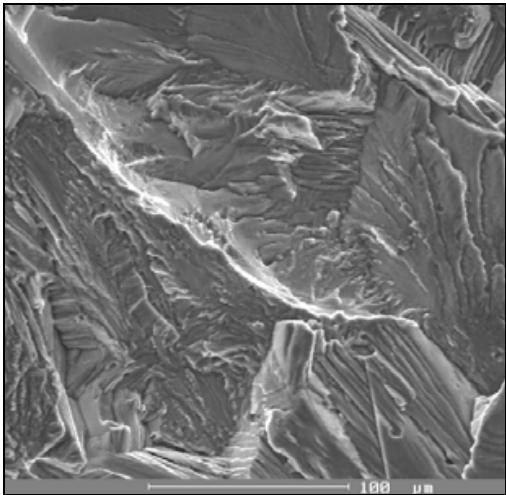
Magnesium alloy AZ 91D was delivered as casting with characteristic casting defects which influenced the fatigue crack initiation, their growth, possibly stop. Amount of casting defects depended on the place of specimen's taking (Fig. 22, 23, 24). The highest amount of casting defects was observed on the specimens taken from the plate middle (Fig. 23), which occurred not only on the surface (Fig. 23a) but also within whole section (Fig. 23b). The casting defects extended to surface of testing bars (Fig. 22a, 23a, 24a) were place of fatigue crack initiation, rarely there were undersurface defects. There were observed not only fatigue failure but also fissile and ductile failure (Fig. 23b) as a consequence of local overload in the proximity of defects. Casting defects occurred very often and sometimes formed large



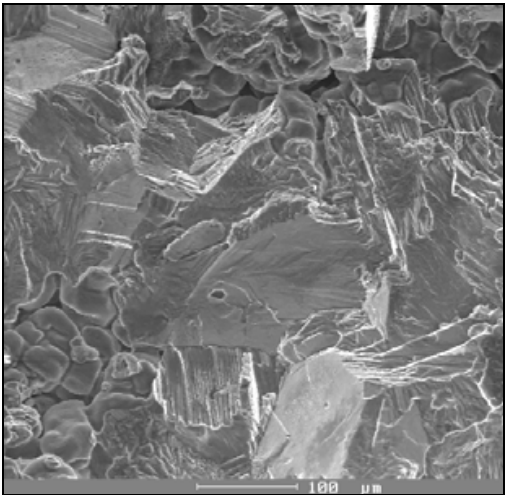
(a) fatigue crack initiation



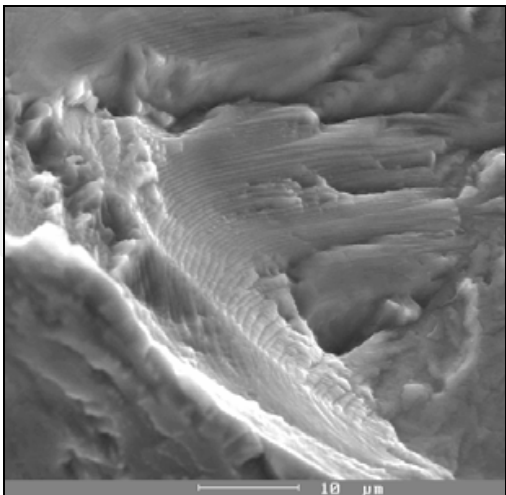
(a) fatigue crack initiation



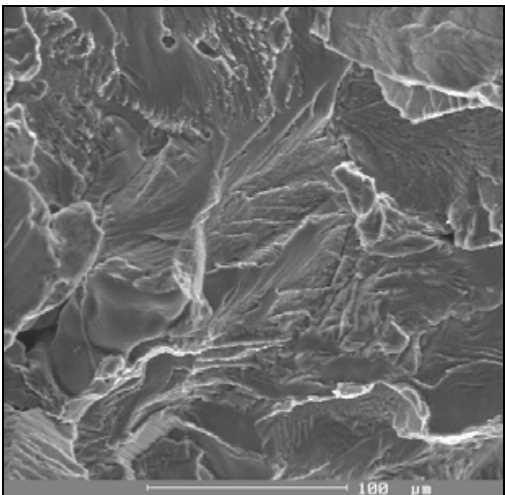
(b) fatigue failure



(b) casting defects, mixed mode of failure



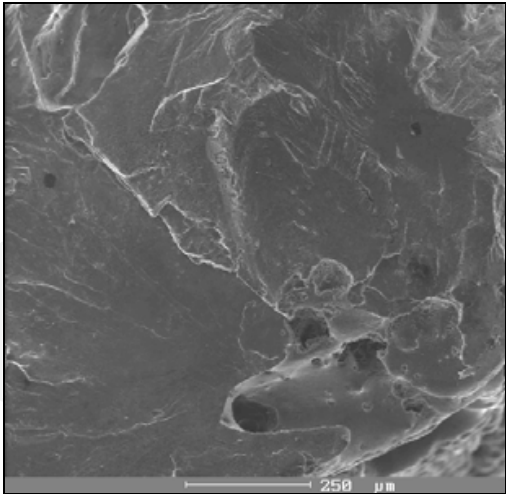
(c) ripples



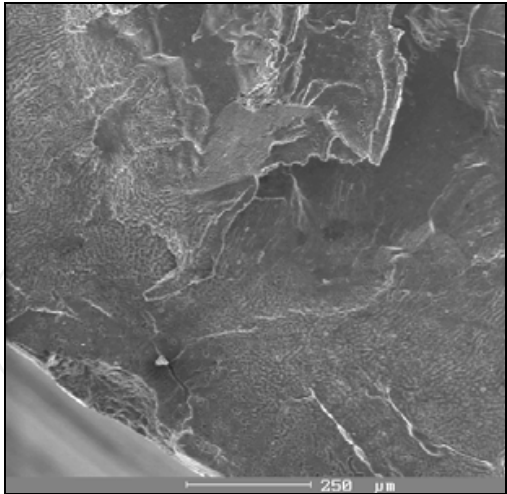
(c) fatigue failure

Fig. 22. Magnesium alloy AZ 91D, the plate edge, S.E.M.

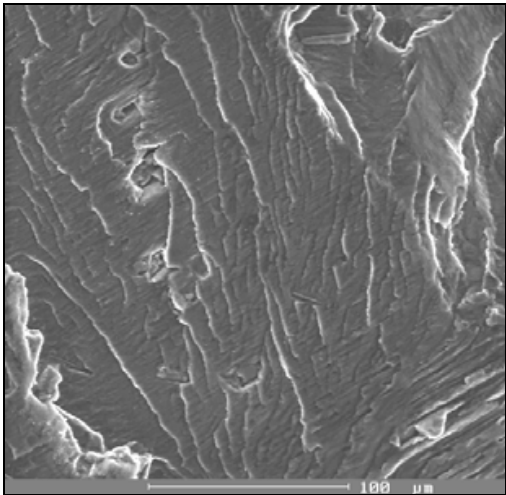
Fig. 23. Magnesium alloy AZ 91D, the plate middle, S.E.M.



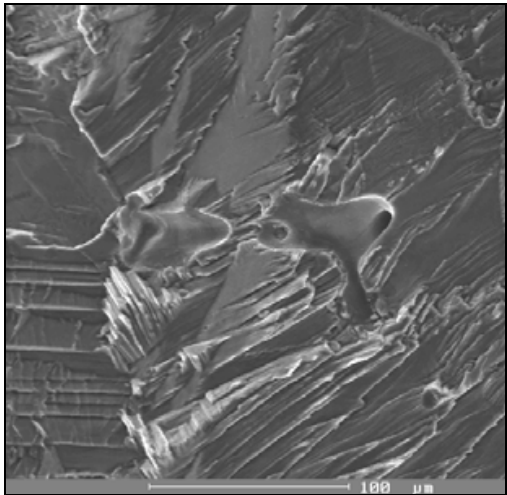
(a) fatigue crack initiation



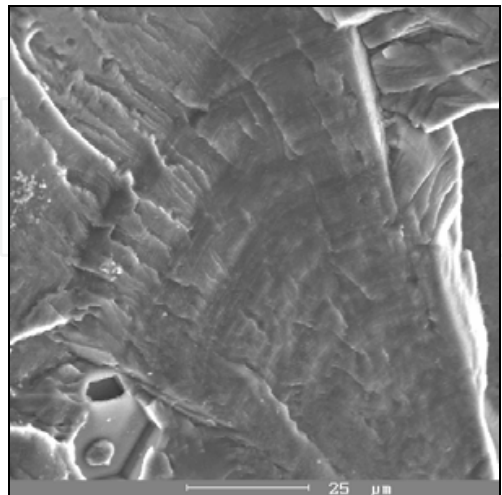
(a) fatigue crack initiation



(b) fatigue failure

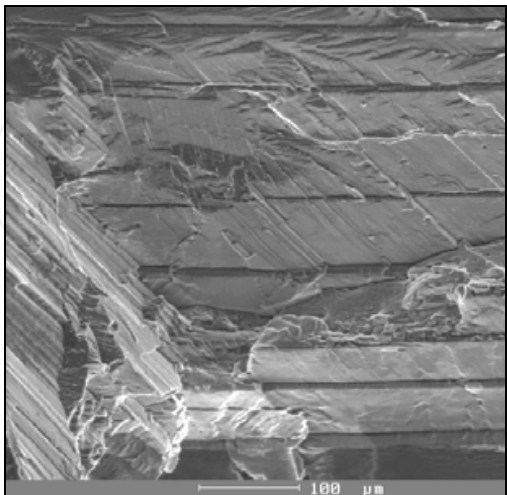


(b) ripples



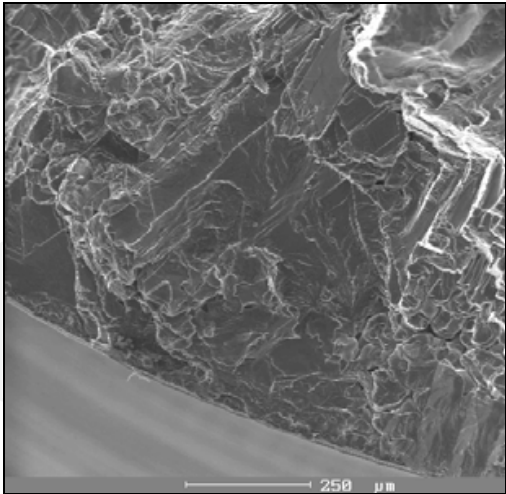
(c) ripples

Fig. 24. Magnesium alloy AZ 91D, block, S.E.M.

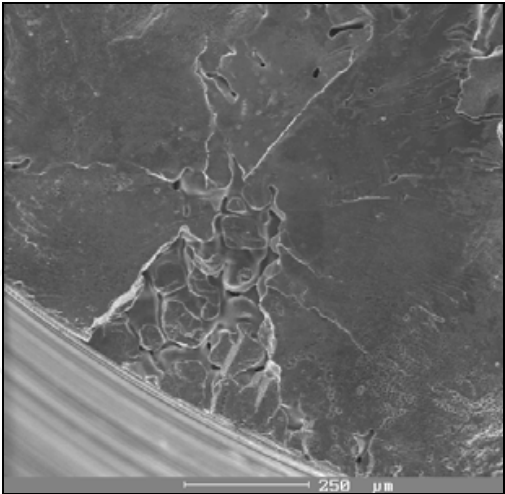


(c) twins

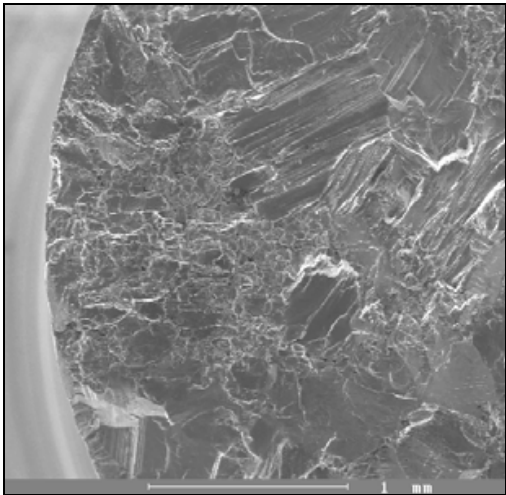
Fig. 25. Magnesium alloy AZ 63HP, the plate edge, S.E.M.



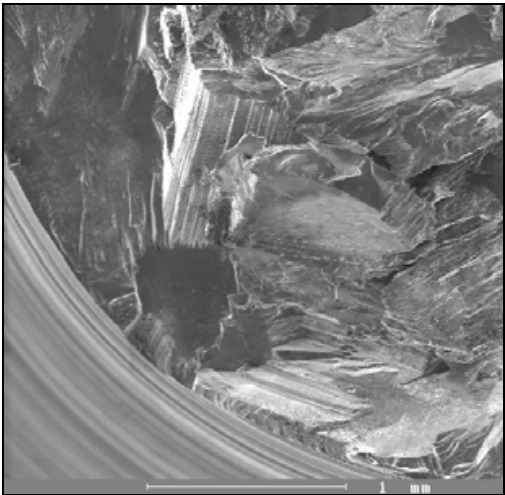
(a) fatigue crack initiation



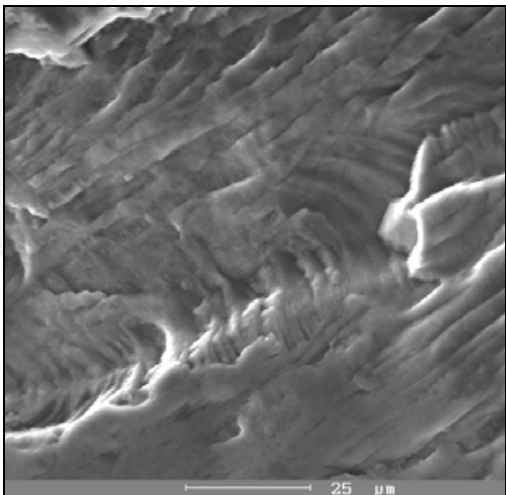
(a) fatigue crack initiation



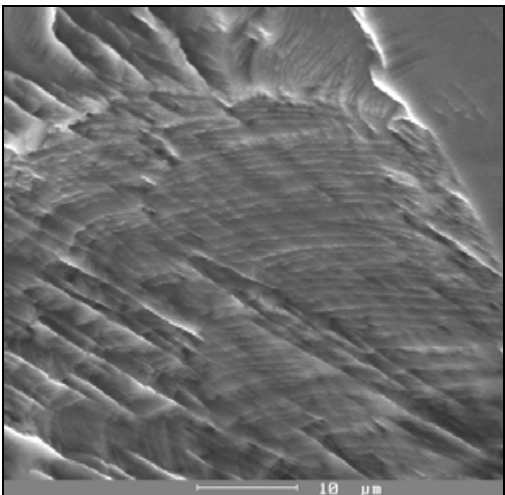
(b) fatigue crack initiation from two places



(b) intercrystalline fissile failure



(c) ripples



(c) ripples

Fig. 26. Magnesium alloy AZ 63HP, the plate middle, S.E.M.

Fig. 27. Magnesium alloy AZ 63HP, the block, S.E.M.

network. Parts of fracture surfaces which showed fatigue failure (Fig. 22b, 23c, 24b) had mostly transcrystalline character and intercrystalline failure made only negligible part. Despite relief's fracture there were possible to observe the fine ripples (Fig. 22c, 24c). Scatter of results at the same stress level was influenced by character of the structure and presence of casting defects.

Fractographic analysis of fracture surfaces carried out on the testing bars taken from the magnesium alloy AZ 63HP showed that fatigue cracks were initiated from the surface of all testing bars. Amount of voids situated on the surface depended on the place of specimen's taking. Presence of the voids on the specimens taken from the plate edge and the block was rare but on the specimens taken from the plate middle they were observed within whole fracture surface. Casting defects were mostly microscopically small but they served as an initiation place of fatigue cracks (Fig. 25a, 26a, 27a). On the fracture surfaces there were possible to observe fatigue crack initiation from two (Fig. 26b) or more places. Fatigue crack growth had mainly transcrystalline mode and there were visible the fine ripples on the investigated surface (Fig. 25b, 26 c, 27c). Fracture surfaces had generally mixed mode with not only the transcrystalline fatigue failure but also intercrystalline fissile failure (Fig. 25b, 27b). In some cases, fatigue crack stopped in the places of casting defects. On the testing bars taken from the plate edge, there were observed the twins (Fig. 25c) which pointed up during the fatigue crack growth as a consequence of either hexagonal lattice deformation or influence of local weakening of material by network of casting defects.

3.3 Simulation of fatigue crack growth in magnesium alloy AZ 91D

Fatigue crack growth in magnesium alloy AZ 91D was simulated using finite-element software ADINA (Automatic Dynamic Nonlinear Analysis) which is suitable for solving large variety of problems. Reliability of modeling is in greater rate supplied by the accuracy in material properties, boundary conditions and last but not least in modeling of proper material behavior at crack tip including singularity if zero radius is presented. Linear and nonlinear fracture mechanics analysis can be performed with ADINA system including computation of conservation criteria (J-integral, energy release rate) in 2D and 3D finite element models. Two different numerical methods are available for the computation of the conservation criteria – the line contour method and the virtual crack extension method. The fracture mechanics allows performing an analysis with only one crack however. The crack line or surface can be located on the boundary or inside of the finite element model.

ADINA is thus fully capable of solving fracture mechanics problems in general with large amount of options in stack under various loading conditions or thermal conditions utilizing wide variety of material models. Also there is the ability to model rupture criteria and thus it is possible to model material damage caused by cavities or impurities and its progression under cyclic load.

The microstructure of the material represented by tightly packed grains was modeled by using the finite-element software ADINA. The geometry of each grain was modeled by Pro/Engineer software and was exported as a plain surface in IGES file to ADINA, where a 2D dynamic analysis was performed. For the analysis each surface representing individual grain of the microstructure was discretized using finite element mesh. In this case quadratic elements were used, which means that unknown quantities were approximated by a polynomial of second order inside of each element. Due to large gradients in secondary fields, it is necessary to use very fine discretisation in the vicinity of the crack to achieve reasonable accuracy. The only factor limiting the fineness of the mesh is of course available

hardware, but for extremely fine mesh a lower numerical stability can be expected. Multi-linear plastic material model was used in the simulation. The properties of the alloy were obtained experimentally as a dependence of displacement of the specimen on the applied force. Afterward the stress-strain curve was imported into ADINA and allocates each element. The analysis was performed by using large deformations and large displacements incorporated into the mathematical model.

Each grain was considered as a standalone body and contact conditions between each pair of grains were implemented. In the microstructure model a stress concentrator was made (Fig. 28). Issue of damage propagation of materials in the microstructure is considerable demanding for the exact model. It is because of some effects are manifested in the atomic structure and they can be described by the continuum mechanics only by certain optimal conditions or on the base of experimental measures, eventually by other specific numerical methods. Because of this, the mesh in the vicinity of the stress concentrator has to be very fine (Fig. 29). On the boundaries was applied a cyclic load with amplitude 30 MPa and with frequency 25 Hz in a pull-push fashion.

The load amplitude by which the propagation of micro-failure occurs is fully dependent on non-homogeneity of the material. A redistribution of stress was influenced by the cyclic nature of the applied load. Even though the stress is applied in uniform manner on the structure, it does not act in the same way on each grain in the structure. Most of the stresses are cumulated in the region with certain non-homogeneity in the microstructure. In this case an artificially created cavity acts as a concentrator. The propagation of material damage was governed similarly to crack propagation, where a plastic zone (Fig. 30) is created in the vicinity of the crack tip in which a plastic strain is accumulated due to cyclic loading.

The deformation process at the crack tip depends significantly on the mechanical properties of the material and on the environment in which the loading occurs. All, limited plastic deformation, equal values of intensity factor and equal coefficients of asymmetry of the

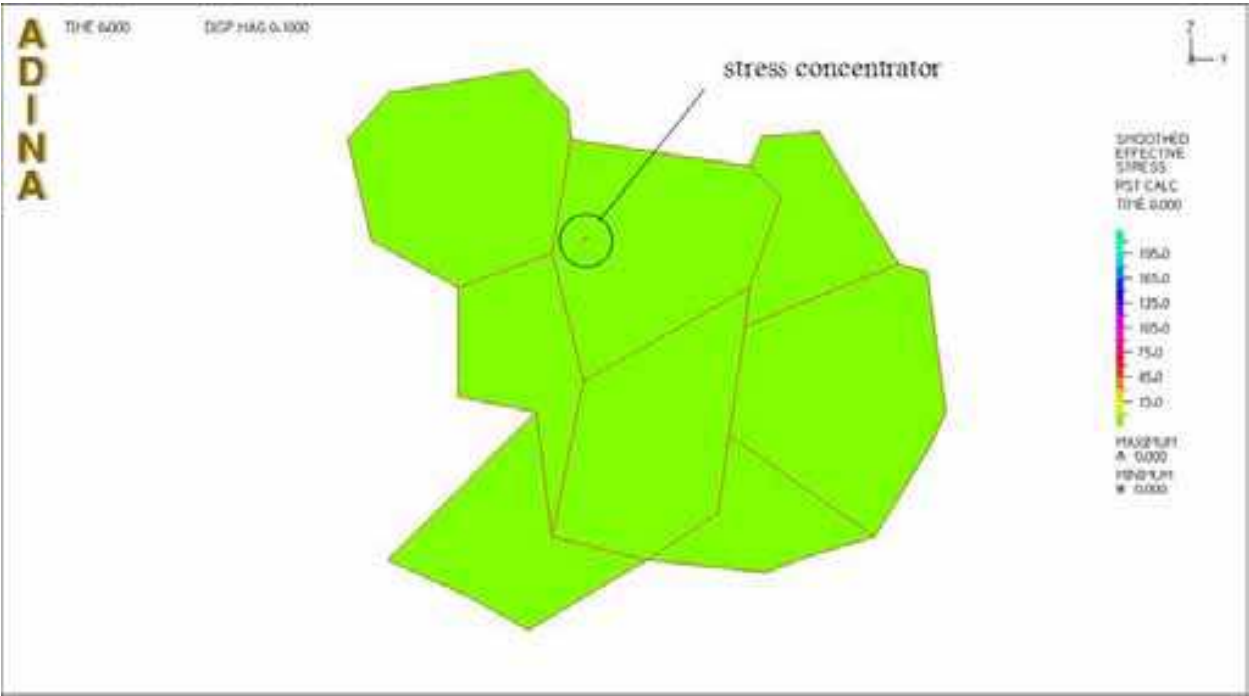


Fig. 28. Model of the microstructure with artificial notch before load

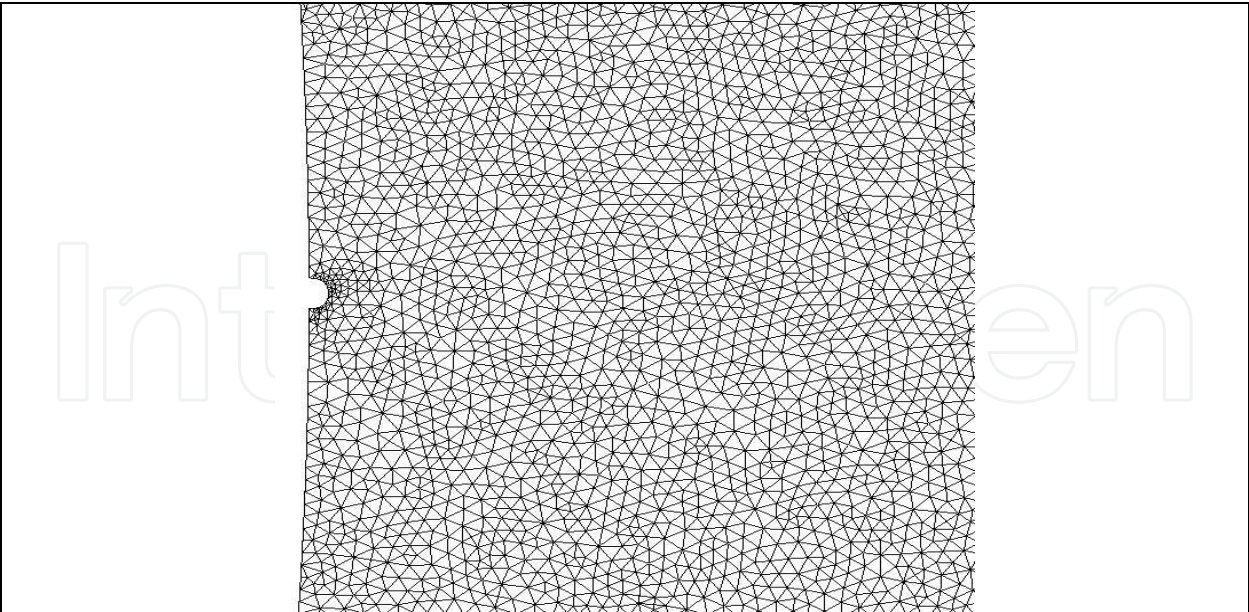


Fig. 29. Mesh in the surrounding of the stress concentrator



Fig. 30. Plastic zone at the crack tip

cycle do not guarantee the same magnitude and form of plastic zone ahead of the crack tip. Once the critical value of the plastic strain is reached in the vicinity of the crack tip, a material damage occurs and the crack propagates (Fig. 31). The crack propagation occurs in the direction of maximal shear stress and its direction gradually changes into direction perpendicular to the direction of applied load. The orientation of main stresses inside of each grain is changing depending on the orientation of the grains, on their shape and on the spread of the damage. The crack acts upon this by changing the direction on the grain boundaries, but due to the damage in the grain can do so even inside of the grain.

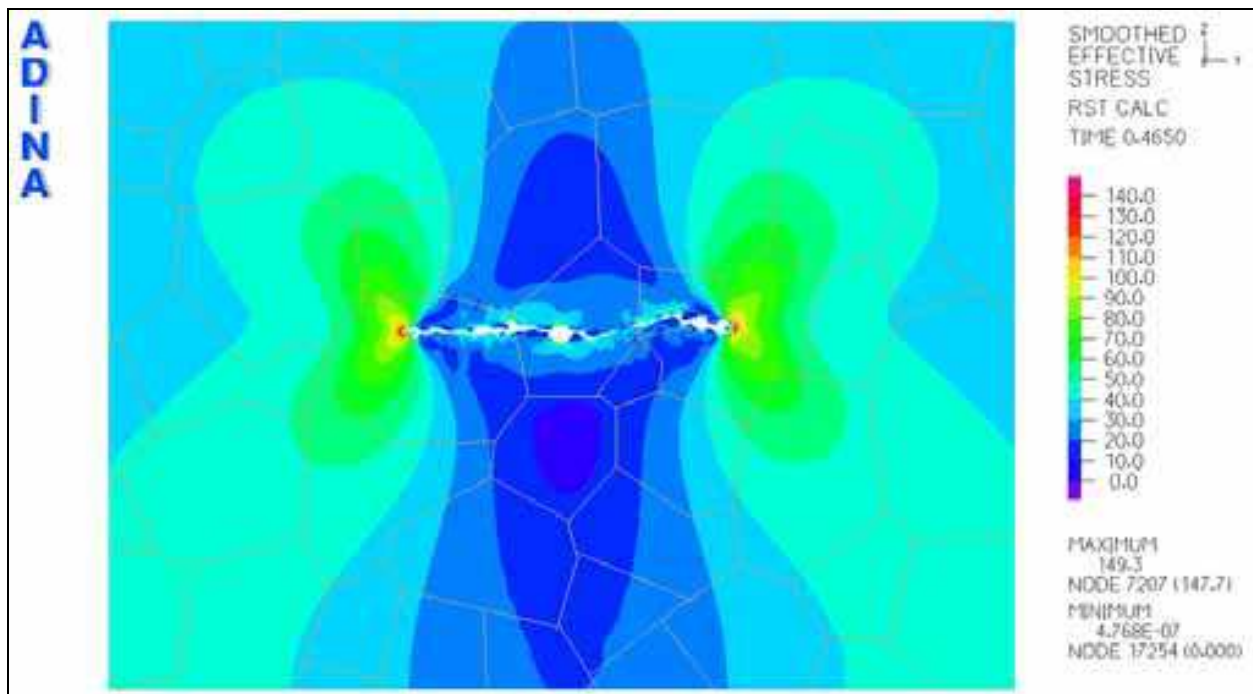


Fig. 31. Fatigue crack growth in magnesium alloy AZ 91D by ADINA

4. Discussion

The results of fatigue test carried out in magnesium alloys AZ 91D and AZ 63HP under high frequency cyclic loading as well as simulation of fatigue crack growth in Mg – alloy AZ 91D are comparable to results of authors mentioned in this chapter.

The initial stage of fatigue is so-called crack-free stage, where the dislocation density increases and different dislocation structures may be generated by micro-plastic deformation. Interactions between dislocations and other structural constituents influence the macroscopic properties (e.g. hardening, softening). This cyclic behaviour during the crack-free stage strongly depends on the initial microstructure and therefore the different magnesium alloy systems and their heat treatments have to be considered to evaluate the cyclic behaviour during fatigue. At first, cyclic hardening was observed in pure magnesium. This effect was also found in some magnesium alloys, which are mainly based on the Mg-Al or Mg-Li systems. The attention is drawn to different heat treatment and their microstructures. In the as-cast (F) and dissolving annealing (T4) usually cyclic hardening occurs, which can be generally attributed to the increase of dislocation density during microplastic deformation. On the contrary, age-hardened alloys show a non-uniform behaviour: the cyclic loading can either lead to hardening or softening, depending on the type of the precipitates. Age-hardened magnesium alloys based on the Mg-RE or Mg-Zn system tend to show cyclic softening due to the presence of coherent precipitates. These precipitates can easily be cut by dislocations, therefore reducing the size of the precipitates, leading to cyclic softening. In contrary, age-hardened magnesium alloys based on the Mg-Al system form incoherent precipitates, which are difficult to cut by dislocations and therefore stable during cyclic loading. Owing to the fact that these precipitates are not efficient to pin dislocations, the cyclic hardening effect of the Mg-Al based alloys seems to be mainly based on the increment of dislocation density. This cyclic hardening effect happens

within approximately the first 10 000 cycles. A generalization of the cyclic behaviour of magnesium alloys is not possible due to the differences in microstructure of the alloy systems and their heat treatment (Potzies & Kainer, 2004).

Like in the other metals, fatigue cracks in magnesium alloys also initiate at slip bands developed by cyclic micro-plastic deformation. The deformation modes of hexagonal structures are rather complex compared to the cubic system. Due to the hexagonal structure of magnesium, dislocation movement at room temperature predominantly occurs in basal slip (0001) planes in the $\langle 1120 \rangle$ directions, while pyramidal slip in $\{1011\} \langle 1120 \rangle$ and prismatic slip in $\{1010\} \langle 1120 \rangle$ is more favourable at higher temperatures. An alternative non-basal deformation mode in hcp structures is the twinning in $\{1012\}$, $\{1011\}$, $\{1122\}$ and $\{1121\}$ - planes, where $\{1012\}$ -twinning is the most common in magnesium. Twinning is an important deformation mechanism in (uniaxial) monotonic deformation but also concerning cyclic micro-plastic deformation during fatigue.

The appearance of fatigue slip bands is only noticed in defect-free material, and despite their good castability, magnesium alloys tend to contain casting defects. The formation of casting defects often depends on the solidification morphology, which in the case of magnesium alloys is mainly endogenously, due to the large solidification range. The large solidification range of most magnesium alloys leads to a formation of microshrinkage, which is additionally favoured by the dendritic grain structure. Another reason for the formation of casting defects may lie in the processing route of the high pressure die casting, which is primarily used for many magnesium alloys. Due to the high casting speeds, the melt flow as non-lamellar and air can be entrapped causing porosity when the melt solidifies. As a consequence, high stress concentrations at casting defects initiate fatigue cracks instead of the afore-mentioned fatigue slip bands. In the presence of casting defects like pores or microshrinkage the crack initiation stage can be reduced to a negligible extent, reducing the lifetime of the component altogether. On the other hand, in defect free material the crack initiation stage - especially at lower stresses - is significantly greater than the crack propagation stage and can be up to 90 % of the total fatigue life. An additional important factor which has to be considered for crack initiation is the condition of the surface and edge layer of the specimens. As already well known, as-cast material usually tends to show higher fatigue lives than machined specimens due to the fine grain edge layer which is removed during the machining.

As it is depicted in Fig. 15 and 16, there are observed two areas of investigated results (area I and II) dependent on number of cycles. There are considered different micromechanisms of failure, surface fatigue crack initiation and undersurface fatigue crack initiation (Mayer, 1998). Fatigue crack initiation in the gigacycle regime seems to occur essentially inside the bars and not at the surface as is observed for shorter lives. So we can model three types of crack initiation in a cylindrical bar with a polished surface depending on whether it is low-cycle (1.10^4 cycles), megacycle (1.10^6 cycles) or gigacycle (1.10^9 cycles) fatigue. For the smallest number of cycles to rupture, the crack initiation sites are multiple and on the surface, while at 1.10^6 cycles, there is only one initiation site, but, for the higher numbers of cycles-to-failure, the initiation is located at an internal zone. An explanation of this phenomenon is that cyclic plastic deformation in the plane stress condition becomes very small in the gigacycle regime. In this case, internal defects or large grain size play a role, in competition with surface damage. The effect of environment is quite small in the gigacycle regime as the initiation of short cracks is inside the bars. The surface plays a minor role

especially if it is smooth. Inclusion can be active crack initiation sites, especially if the load ratio is high. The porosities can initiate a crack in competition with inclusions, especially when the load ratio is low, particularly in pull-push (Bathias, 1999). Another explanation of fatigue crack initiation in gigacycle regime is by stress concentration between two or more grains where a long grain boundary is located perpendicular to the pull stress and therefore it works as an internal notch.

After the crack initiation, the short crack usually advance in an angle of 45° to the load and are strongly influenced by the microstructure, e.g. grain boundaries, and the orientation of the basal (0001) slip bands. During propagation the cracks grow and change their orientation, being perpendicular to the load. The fatigue crack propagation can be either trans- or intercrystalline. In the as-cast (F) of AZ 91, for example, the brittle intermetallic $\text{Al}_{12}\text{Mg}_{17}$ at the grain boundaries favours interdendritic cracking. Additionally, high crack tip driving forces tend to promote crack propagation through the $\text{Al}_{12}\text{Mg}_{17}$ phase, while lower loads assist crack propagation through the primary α -Mg grains. The crack growth is additionally assisted by the connection of different microcracks or – especially in material with casting defects – cracks, which developed between pores or microshrinkage (Potzies & Kainer, 2004).

Concerning the crack propagation rate, magnesium and its alloys in general, show a very low fracture toughness, which therefore promotes a higher crack propagation rate than in other light metal. Furthermore, the crack propagation rate strongly depends on the individual microstructure (type of alloy, heat treatment) and the micro structural constituents, e.g. precipitates. In age-hardened (T6) ternary Mg-Li based alloy and Mg-Nd and Mg-Zn based alloys the precipitates formed can cause a decelerating effect on the crack propagation, while in the age-hardened (T6) and as-cast (F) magnesium alloy AZ 91 the $\text{Al}_{12}\text{Mg}_{17}$ intermetallic, rather increases the crack propagation rate. To improve the fatigue crack propagation resistance of the Mg-Al based alloys, additional elements can be used to form intermetallics with higher fracture toughness. Yttrium and neodymium added to AZ 91 are found to show a beneficial effect on the fracture toughness, leading to the reduction in the fatigue crack propagation rate. Beside, different mechanical surface treatments (e.g. shot-peening, deep-rolling) can be used to modify the edge layer. The increased near-surface dislocation density and the implemented compressive residual stresses significantly reduce the crack propagation rate, increasing the fatigue lives although the crack initiation is accelerated due to the increased surface roughness (Potzies & Kainer, 2004).

Fatigue crack propagation of long cracks is customarily divided in three regimes. Regime A or near-threshold is of great practical importance and it is characterized by complex testing procedures and by the influence of many experimental and material factors. Regime B or Paris's regime has been extensively studied because of its usefulness for the damage tolerant approach to the fatigue design of aerospace structure (Kelemen, 2004). Regime C characterizes the rapid crack extension to final fracture. The main characteristics that differentiate Regime A and B are extension to final fracture. The near-tip plasticity and its relationship with a typical material microstructural feature, such as the average grain size, can be used to discriminate between regimes A and B. The near-threshold regime in metals is generally associated with a crack tip plasticity largely confined to select crystallographic planes with a reversed-shear mode of growth. Crack deflections due to microstructural heterogeneity can lead to mixed-mode displacements on the microscopic level and a faceted fracture surface. These displacements cause mismatch between upper and lower crack faces

which in turn results in a positive closure load. Here attention is devoted to the roughness-induced crack closure (RICC) because it is strongly influenced by the material microstructure and it is associated to a zigzag crack pattern. RICC is promoted by: a) low stress intensity factor levels where the plastic zone is smaller than the average grain diameter, b) small crack opening displacements (e.g. low ΔK and low R-ratios) of a size comparable to surface asperities, c) coarse grained microstructures, d) periodic deflections of the crack due to grain boundaries, second-phase particles and composite reinforcement, e) enhanced slip irreversibility. Fatigue crack paths in a coarse-grained material become complicated even at relatively high stress intensities. The resulting crack tortuosity involves several mechanisms and tends to reduce the effective stress intensity range, ΔK_{eff} , below the nominal applied range, ΔK .

RICC limits the minimum stress intensity, hook or 'lock-up' mechanisms limit the maximum stress intensity and branching produces true elastic shielding. Tortuosity also increases the ratio of the true length to that projected on the plane of the stress axis reducing the energy release rate. The crack path is a result of a series of mechanisms associated with different stages of fatigue crack growth. When the plastic zone extends over a number of grains due to a high ΔK or to a fine-grained material, quasi continuum mechanisms are operative. A rectilinear Mode I crack path, also termed a Stage II fatigue crack, occurs during fatigue crack propagation of long cracks. A dual-slip system is active at the crack tip, and the crack growth process involves simultaneous or alternating flow along this slip system.

When crack growth rates are reduced toward threshold conditions specific features can be observed. A stage I crack growth, occurring predominantly by single shear in the direction of the primary slip system, can develop because the plastic zone becomes smaller of the average grain size. Crack propagation is characterized by crack deflection from grain to grain (Nicoletto et al., 2003).

The corrosion fatigue has been tested in different aqueous solutions, but most investigations have been performed with sodium chloride solutions. Generally, the influence of corrosion fatigue shows a significant reduction in fatigue life of magnesium components with different impacts depending on the selected solutions. In the presence of aqueous solutions the fatigue crack initiation, which is more influenced by the corrosive environment than the crack propagation, often starts at cracked regions in the corrosion layer, which mainly consists of magnesium hydroxide. Due to the lower specific volume of magnesium hydroxide compared to the magnesium substrate, the layer fractures easily and corrosion can continue within the voids. These voids can act as additional initiation sites for fatigue failure. To avoid degradation of the surface, special surface treatments or coatings are therefore advisable. Anodizing, chromating or sealing with epoxy resins are possible surface treatments to form protective layers. Additionally, fatigue cracks can also initiate at corrosion pits developed by local galvanic corrosion at precipitates or impurities. These corrosion pits become more effective in high cycle fatigue regimes with low load amplitudes. To avoid local galvanic corrosion, usually high purity alloys (HP) are used. Besides corrosion induced damage of the surface, casting defects, like ores or microshrinkage are very effective origins for fatigue cracks. Despite the additional corrosive attack at these casting defects, the fatigue life is not further reduced compared to the fatigue life in air.

Besides corrosion, elevated temperatures are another critical environment for magnesium alloys and lead to lower mechanical properties already of 120°C and above. The results show a significantly decreasing fatigue life with increasing temperature, due to greater plastic strain amplitudes, which promotes the initiation of fatigue cracks (Potzies & Kainer, 2004).

5. Conclusion

Magnesium alloys show a high specific strength and are therefore increasingly used for light-weight constructions in automobile industry. Any moving causes vibrations leading to cyclic loading in the components. To predict the behaviour of the material under the influence of cyclic loading it is vital to understand the fatigue behaviour of magnesium alloys.

The technique of ultrasonic fatigue is especially appropriate to perform fatigue experiments in very high-cycle regime of $1 \cdot 10^9$ and more within reasonable testing times, whereas extremely long testing times (months or years) would be needed with all other conventional testing equipment.

To improve the fatigue behaviour of magnesium alloys, two different main approaches are possible: surface modification to improve the fatigue resistance (mechanical surface treatment) and /or corrosion resistance (coating), improvement of the bulk material to decelerate crack initiation (avoid casting defects) or to reduce the crack propagation rate (increase fracture toughness).

The first approach can be realized by techniques of mechanical surface hardening treatments, which improve the fatigue resistance by introducing compressive residual stresses into the surface layer. The compressive residual stress and the increment of surface hardness decelerate the process of fatigue crack initiation by reducing the dislocation movement. By using roller burnishing even the corrosion fatigue resistance can be improved.

Another possibility to decelerate the fatigue crack initiation, especially when the magnesium components are exposed to a corrosive media, is the use of surface coatings. These coatings reduce the corrosive attack and therefore the formation of corrosive induced cracks and corrosion pits, which often act as fatigue crack initiation sites.

Considering the second approach by improving the bulk material, the focus should be set on reducing the casting defects by using new or optimized casting techniques. Advanced or new processes, like vacuum pressure die casting or semi-solid processing respectively, enable a reduction of porosity in cast components, increasing the fatigue life. Reducing the porosity, additionally decreases the scatter and therefore improving the reliability.

Besides reducing casting defects, adding certain alloying elements to increase the fracture toughness is a further option to improve the fatigue behaviour of magnesium alloys. Yttrium and neodymium have been found to increase the fracture toughness of AZ 91 and reduce the crack propagation rate. Though a possible option, this effect is less pronounced, compared to minimizing the porosity.

Depending on the demand of certain mechanical properties and the exposure to detrimental environments, several opportunities are available to improve the fatigue behaviour and increase the fatigue life of magnesium alloys (Potzies & Kainer, 2004).

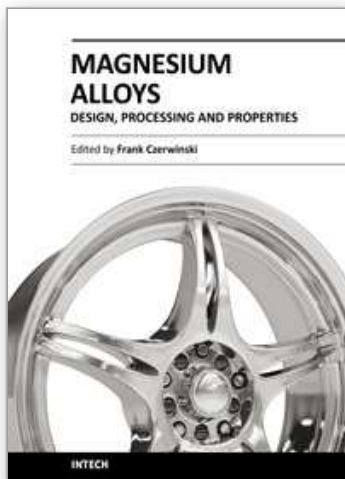
To apply the full potential of weight reduction by using magnesium alloys, especially in transportation applications, further investigations are still necessary to fully understand the fatigue behaviour of magnesium alloys and to transfer the knowledge for further alloy development and component design.

6. References

- Avedesian, M. M. (1999). *ASM Specialty Handbook, Magnesium and Magnesium Alloys*, Michael Avedesian and Hugh Baker, ISBN 0871706571
- Bathias, C. (1999) There is no infinite fatigue life in metallic materials, *Fatigue Fract Engng Mater Struct*, Vol. 22, No. 7, (July 1999), pp. 559-565, ISSN 8756-758X
- Bursk, R.S.(1987). *Magnesium Products Design*, Marcel Dekker, New York.
- Cllaper, R. B. & Watz, J. A. (1956). Determination of Fatigue Crack Initiation and Propagation in a Magnesium Alloys, In: *ASTM STP 196*, 1956, p. 111
- Goodenberger, D. (1990). *Fatigue and Fracture Behavior of AZ91E – T6 Sand Cast Alloy*. Masters's thesis, The University of Iowa
- Ishikawa K.; Kobayashi, Y. & Ito, T. (1995). Characteristics of Fatigue Crack Propagation in Heat Treatable Die Cast Magnesium Alloy. *Proceedings of 124th TMS Annual Meeting*, pp. 449-460, Las Vegas, 1995, USA
- Ishikawa, K.; Kobayashi, Z.; Kaneko, T. & Shibusawa, T. (1997). Precipitated Structures and Mechanical Properties of AZ 91D Magnesium Alloy. *Nippon Kinzoku Gakaishi - Journal of the Japan Institute of Metals*, Vol. 61, No. 10, (June, 1997) 1031-1036, ISSN 0021-4876
- Ishikawa, K.; Kobayashi, Y. & Kentarou, K. (2001) Abstract Endurance Limit and Fatigue Crack Propagation of Magnesium Alloys, *Proceedings of Fatigue in the Very High Cycle Regime*. pp. 199-205, Wiena, June 2001, Austria
- Kaya, A.A. ; Uzan, P. ; Eliezer, D. & Aghion, E. (2000). Electron microscopical investigation of as cast AZ 91D alloy. *Materials Science and Technology*, Vol. 16, No. 9 (September 2000) 1001-1006, ISSN 0267-0836
- Kelemen, M. (2004) Ground Search and Rescue Service, *Proceedings of Aerospace medicine and 1st Annual Intern. Forum on Disaster Medicine*, pp. 38, Košice, June 2004, Košice
- Laird, C. & Charsley, P. (1982) Strain Rate Sensitivity Effects in Cyclic Deformation and Fatigue Fracture. *Proceedings of Ultrasonic Fatigue*, Champion; Pa ; October 1981. pp. 187-205
- Lynch, S. P. (1998) Environmentally Asisted Cracking: Overwiev of Evidence for an Adsorption – Induced Localised – Slip Process. *Acta Met.*, Vol. 36, No. 10, (October 1988) 2639 –2661, ISSN 1359-6454
- Makar, G. L.; Kruger, J. & Sieradzki, K. (1993) Stress Corrosion Cracking of Rapidly Solidified Magnesium – Aluminium Alloys. *Corrosion Sci.*, Vol. 34, No. 8 (August 1993), 1311-1323, ISSN 0010-938X
- Mayer H.; Rösch, R.; Lipowsky, H.; Zettl, B.; Papakyriacou, M. & Stanzl-Tschegg, S.E. (1997). Fatigue Properties of High Pressure die Cast Magnesium Alloys, *Proceedings of Magnesium 97*, pp. 145 – 150, Dead Sea, June 1997, Israel
- Mayer, H. (1998) Application of Ultrasonic Frequencies in Fatigue. *Kovové materially-Metallic Materials*, Vol. 36, No. 3, (1998), 213-219 , ISSN 0023-432X
- Mayer, H. ; Lipowsky, H. ; Papakyriacou, M.; Rosch, R.; Stich, A. & Stanzl-Tschegg, S. (1999) Applications of Ultrasound for Fatigue Testing of Lightweight Alloys, *Fatigue Fract.Engng. Mater.Struct.*, Vol. 22, No. 7, (July 1999) 591-599, ISSN 8756-758X
- Nečas, P. & Kelemen, M. (2010). *War on insecurity: calling for effective strategy!*, The centre of educational literature, ISBN 978-611-01-0023-6, Kiev

- Nicoletto, G.; Konečná, R. & Pirondi, A. (2003) Fatigue Crack Paths in Coarse – grained Magnesium. *Proceedings of Fatigue Crack Paths*. Pp. 1-8, Parma, September 2003, Italy
- Papakyriacou, M. ; Mayer, H. ; Pypen, C. ; Jr H.P. & Stanzl-Tschegg, S.E.(2001) Influence of Loading Frequency on High – Cycle Fatigue Properties of b.c.c. and h.c.p. Metals, *Material Sci. Eng. A*, Vol. 308, No. 1-2, (June 2001) 143-152, ISSN 0921-5093
- Potzies, C. & Kainer, K.U. (2004) Fatigue of Magnesium Alloys. *Advanced Engineering Materials*, Vol. 6, No. 5, (May 2004) 281-289, ISSN 1438-1656
- Puškár, A.; Bokúvka, O.; Palček, P. & Meško J. (1987) Inštrumentalizácia a metodiky únavových skúšok pri ultrazvukovej frekvencii zaťažovania, *Strojírenství*, Vol. 37, No. 9, 1987, 507-513
- Salama, K. & Lamerand, R.K. (1982) Ultrasonic Fatigue, *Met. Society*, AIME, New York,
- Sander, M. & Richard, H.A. (2006). Fatigue crack growth under variable amplitude loading Part II : analytical and numerical investigations. *Fatigue Fract. Engng. Mater. Struct.*, Vol. 29, No. 4, (april 2006) 303-319I, SSN 8756-758X
- Shibusawa, T ; Kobayashi, Y. & Ishikawa, K. (1997). Fatigue Crack Propagation in Die – cast AZ 91D Magnesium Alloy. *Nippon Kinzoku Gakaishi - Journal of the Japan Institute of Metals*, Vol. 61, No. 4, (September, 1997) 298-302, ISSN 0021-4876
- Stanzl, S.E.; Hollanek, W. & Tschegg, E.K. (1984) Fatigue and Fracture Under Variable – Amplitude Loading at Ultrasonic Frequency, *Advances in Fracture Research*, Ed. S. R. Valuri et al., 3645-3651, Pergamon Press
- Zheng, L.; Yan – Chun, L.; Zhong – Guang, W.; Yue, W. & Zhong – Yang, L. (2000). Influence of Load Frequency and Heat Treatment on Fatigue Crack Propagation Rate of Die – casting Alloy AZ 91HP. *Hangkong Cailia Xuebao – Journal of Aeronautical Materials*, Vol. 20, No. 1, (January, 2000) , 7-20, ISSN 1005-5053

IntechOpen



Magnesium Alloys - Design, Processing and Properties

Edited by Frank Czerwinski

ISBN 978-953-307-520-4

Hard cover, 526 pages

Publisher InTech

Published online 14, January, 2011

Published in print edition January, 2011

Scientists and engineers for decades searched to utilize magnesium, known of its low density, for light-weighting in many industrial sectors. This book provides a broad review of recent global developments in theory and practice of modern magnesium alloys. It covers fundamental aspects of alloy strengthening, recrystallization, details of microstructure and a unique role of grain refinement. The theory is linked with elements of alloy design and specific properties, including fatigue and creep resistance. Also technologies of alloy formation and processing, such as sheet rolling, semi-solid forming, welding and joining are considered. An opportunity of creation the metal matrix composite based on magnesium matrix is described along with carbon nanotubes as an effective reinforcement. A mixture of science and technology makes this book very useful for professionals from academia and industry.

How to reference

In order to correctly reference this scholarly work, feel free to copy and paste the following:

Mariana Kuffova (2011). Fatigue Endurance of Magnesium Alloys, Magnesium Alloys - Design, Processing and Properties, Frank Czerwinski (Ed.), ISBN: 978-953-307-520-4, InTech, Available from:

<http://www.intechopen.com/books/magnesium-alloys-design-processing-and-properties/fatigue-endurance-of-magnesium-alloys>

INTECH
open science | open minds

InTech Europe

University Campus STeP Ri
Slavka Krautzeka 83/A
51000 Rijeka, Croatia
Phone: +385 (51) 770 447
Fax: +385 (51) 686 166
www.intechopen.com

InTech China

Unit 405, Office Block, Hotel Equatorial Shanghai
No.65, Yan An Road (West), Shanghai, 200040, China
中国上海市延安西路65号上海国际贵都大饭店办公楼405单元
Phone: +86-21-62489820
Fax: +86-21-62489821

© 2011 The Author(s). Licensee IntechOpen. This chapter is distributed under the terms of the [Creative Commons Attribution-NonCommercial-ShareAlike-3.0 License](https://creativecommons.org/licenses/by-nc-sa/3.0/), which permits use, distribution and reproduction for non-commercial purposes, provided the original is properly cited and derivative works building on this content are distributed under the same license.

IntechOpen

IntechOpen